Babeș-Bolyai University
Faculty of Chemistry and Chemical Engineering
Supramolecular Organic and Organometallic
Chemistry Centre

Contributions to the chemistry of organotin(IV) and tin(II) complexes with a pyrazolyl-based selenolato ligand

PhD Thesis summary

Melinda-Erika Tamas

Scientific Advisor:
Prof. Dr. Anca Silvestru

Cluj-Napoca
2025

Review committee

Scientific advisor: Prof. Dr. Anca Silvestru
Faculty of Chemistry and Chemical Engineering,
“Babeş-Bolyai” University, Cluj-Napoca, Romania

Chair:

Prof. Dr. Tiberiu Frenţiu
Faculty of Chemistry and Chemical Engineering,
“Babeş-Bolyai” University, Cluj-Napoca, Romania

Reviewers:

Conf. Dr. Albert Soran
Faculty of Chemistry and Chemical Engineering,
“Babeş-Bolyai” University, Cluj-Napoca, Romania

CSI Dr. Otilia Costişor
“Coriolan Drăgulescu” Institute for Chemistry, Timişoara, Romania

Prof. Dr. Cecilia Cristea
Faculty of Farmacy,
“Iuliu Haţieganu” University of Medicine and Farmacy,
Cluj-Napoca, Romania

Table of contents

1. Introduction

Tin has been mentioned since the beginning of the Bronze Age (around 3000 BC)[1] and is the Earth's 49th most abundant element. It is a soft, malleable, and highly crystalline post-transition metal element, with the electronic configuration [Kr]$4d^{10}5s^{2}5p^{2}$, situated in group 14 of the Periodic Table.

Tin displays two oxidation states (+2 or +4) in both inorganic and organometallic compounds. The derivatives containing divalent tin are called stannous, while the compounds containing tetravalent tin are called stannic species. The stannous state typically uses 5*p* orbitals for bonding and the 5*s* electrons as a nonbonding pair, thus adopting an angle X−Sn−X of 90-100°. In stannic derivatives, the metal centre is sp^3 hybridised with a tetrahedral geometry and has vacant *5d* orbitals, which can be involved in interactions, thus giving rise to structures with higher coordination numbers.[2]

Standard Oil Development Co. was the first to obtain a patent in 1932 for the industrial application of an organotin compound, specifically using tetraalkyltin derivatives to stabilise transformer oils.[3] From that point, various application forms were studied for the organotin compounds, like PVC stabilizers,[4] biocides (fungicides, pesticides, antifouling agents),[5] Li-ion batteries[6] or in organic chemistry, as reducing agents (tin II species) or as catalysts in various transformations, e.g. allylation, transmetalation, cross-coupling reactions,[7] and in medicine, as antitumor agents.[8]

On the other hand, selenium is a chalcogen element, with the atomic number 34 and an electronic configuration [Ar]$3d^{10}4s^{2}4p^{4}$, situated in group 16 of the Periodic Table. Organoselenium derivatives can have various oxidation states in organoselenium compounds, namely +1 in diorganodiselenides, +2 in diorganoselenides, and +4 in R_nSeX_{4-n} (R = alkyl, aryl; n = 1-3, X = anionic ligand) derivatives. Very importantly, selenium can easily behave either as Lewis acid or as Lewis base, depending on the partner in the reaction. This fact was intensively exploited to obtain various species with a large spectrum of applications.[9,10]

Jöns Jakob Berzelius was the discoverer of selenium, in 1817. He was working in a sulfuric acid factory and observed that reddish deposits formed in the lead chamber while he prepared sulfuric acid.[11] However, the selenium applications were essentially unimportant until 1972, when a discovery was made, namely that selenocysteine, the 21st amino acid, which has the same structure as cysteine but with an atom of selenium in place of the sulfur, was discovered at the active site of glutathione peroxidase (GPx).[12] This prompted extensive research into the structural aspects of organoselenium compounds that affect the antioxidant properties, ultimately leading to the rational development of small molecules exhibiting GPx-like activity.[13]

The studies reported in this work combine the two elements, tin and selenium, in the same molecule, in order to enhance the specific properties and the potential for valuable applications as antitumor agents or as precursors for nanomaterials. The main focus of this thesis is on the synthesis, structural characterization, and study of the potential biological activity of several organotin compounds with organoselenolato ligands. Selected species were also investigated for their thermal behaviour, taking into account the potential as precursors for nanomaterials. The investigations are devoted to three main classes of complexes:

1. Homo- and heteroleptic triorganotin(IV) organoselenolato complexes of types $R_3Sn(SeCH_2CH_2pz)$ (R = Me, ^{n}Bu, Ph, Bn), $[2\text{-}(Me_2NCH_2)C_6H_4](R)_2Sn(SeCH_2CH_2pz)$ (R = Me, ^{n}Bu, Ph) and $[2\text{-}(Me_2NCH_2)C_6H_4]_2(R)Sn(SeCH_2CH_2pz)$ (R = Me, ^{n}Bu, Ph);
2. Diorganotin(IV) organoselenolato complexes of types $[2\text{-}(Me_2NCH_2)C_6H_4](R)Sn(SeCH_2CH_2pz)_2$ (R = Me, ^{n}Bu, Ph), $[2\text{-}(Me_2NCH_2)C_6H_4](R)Sn(NCS)(SeCH_2CH_2pz)$ (R = Me, ^{n}Bu, Ph) and $[2\text{-}(Me_2NCH_2)C_6H_4](R)Sn(SeCH_2CH_2pz)Cl$;
3. Organotin(II) organoselenolates of types $Sn(SeCH_2CH_2pz)_2$ and $Sn(SeCH_2CH_2pz)X$ (X = Cl, NCS);

All the newly synthesised compounds were characterised through multinuclear NMR (^1H, $^{13}C\{^1H\}$, $^{77}Se\{^1H\}$, $^{19}Sn\{^1H\}$) and 2D (H, H-COSY, H, C-HSQC and H, C-HMBC) NMR spectra, mass spectrometry, and elemental analysis. Also, the structures of some compounds, where single crystals could be grown, were investigated by single-crystal X-ray diffraction.

3. Original contributions

3.1. Homo- and heteroleptic triorganotin(IV) organoselenolates

3.1.1. Synthesis and characterisation

The complexes were obtained by splitting the Se−Se bond in degassed absolute ethanol, under argon, with $NaBH_4$. Then, the resulting sodium organoselenolates were reacted in a 1:1 molar ratio with the corresponding homoleptic triorganotin(IV) chloride, as depicted in **Scheme 1**.

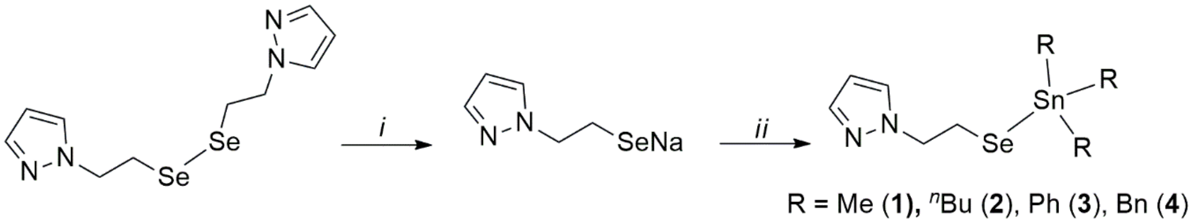

Scheme 1. Synthetic pathway for the preparation of complexes **1-4**. Reagents and conditions: *i)* $NaBH_4$, degassed absolute ethanol at 0 °C, *ii)* R_3SnCl (R = Me, ^{n}Bu, Ph, Bn).

The synthesis method is similar to the homoleptic complexes, but in this case, the resulting sodium organoselenolates were reacted, in a 1:1 molar ratio, with a corresponding heteroleptic triorganotin(IV) chloride as depicted in **Scheme 2**.

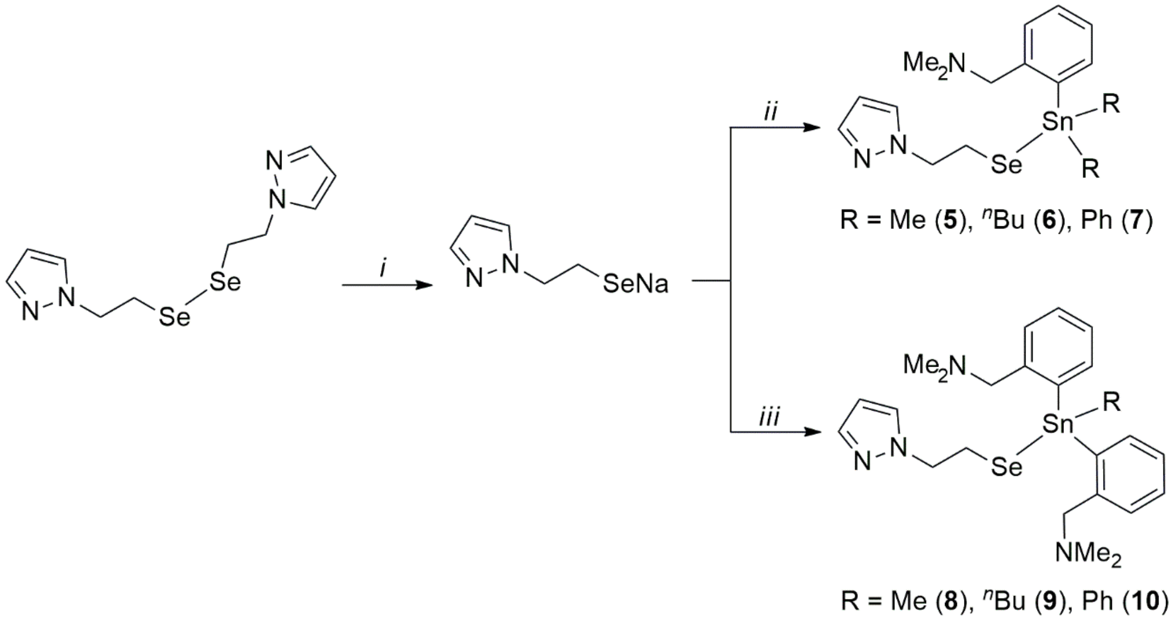

Scheme 2. Synthesis of complexes **5-10**. Reagents and conditions: *i)* $NaBH_4$, degassed absolute ethanol at 0 °C *ii)* $[2\text{-}(Me_2NCH_2)C_6H_4](R)_2SnCl$ (R = Me, ^{n}Bu, Ph), *iii)* $[2\text{-}(Me_2NCH_2)C_6H_4]_2(R)SnCl$ (R = Me, ^{n}Bu, Ph).

Nuclear magnetic resonance (NMR) spectroscopy is one of the principal techniques used to obtain structural information in solution. Compounds **1-10** were characterised by multinuclear NMR (^{1}H, ^{13}C{^{1}H}, ^{77}Se{^{1}H}, ^{19}Sn{^{1}H}) spectroscopy in $CDCl_3$ solutions and the obtained resonance signals in the proton and carbon NMR spectra were unambiguously assigned by 2D NMR experiments (H, H-COSY, H, C-HSQC and H, C-HMBC). The ^{1}H and ^{13}C{^{1}H} NMR spectra consistently display a set of characteristic resonance signals that ensure the existence of the proposed compounds.

In the compared proton NMR spectra of compound **1** and the starting diorganodiselenide, presented in **Figure 1**, all the expected resonance signals of the complex have different chemical shift values compared to the diorganodiselenide. In the aliphatic region of the compared spectra, three signals can be observed. A sharp singlet resonance signal corresponds to the protons in the methyl group, which is accompanied by tin satellites with $^2J_{117\text{SnH}}$ 53.2 Hz and $^2J_{119\text{SnH}}$ 59.8 Hz coupling constants, and two triplet resonance signals corresponding to protons in the non-equivalent methylene groups. In the aromatic region, a triplet and two doublet resonance signals from the pyrazole group are present.

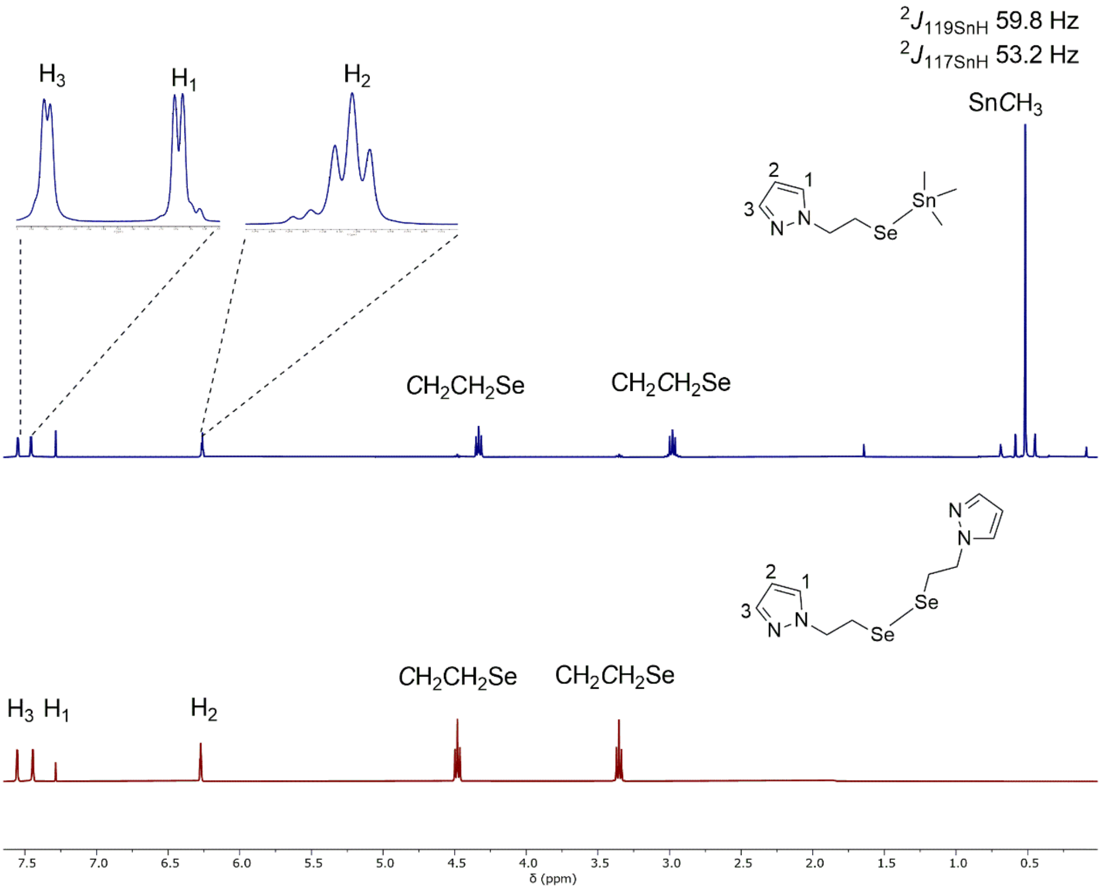

Figure 1. ^{1}H NMR spectra ($CDCl_3$) of compound **1** and the starting diorganodiselenide.

Figure 2 presents the proton NMR spectra of compounds $^{n}Bu_3Sn(SeCH_2CH_2pz)$ (**2**), $[2\text{-}(Me_2NCH_2)C_6H_4](^{n}Bu)_2Sn(SeCH_2CH_2pz)$ (**6**), $[2\text{-}(Me_2NCH_2)C_6H_4]_2(^{n}Bu)Sn(SeCH_2CH_2pz)$ (**9**). In the aliphatic region, all compounds have a triplet and three multiplet resonance signals corresponding to the butyl group present in the molecules. Also, we can observe that $[2\text{-}(Me_2NCH_2)C_6H_4](^{n}Bu)_2Sn(SeCH_2CH_2pz)$ (**6**) has a sharp singlet resonance corresponding to the H_7 protons from the N,N-dimethylbenzylamine group, but compound $[2\text{-}(Me_2NCH_2)C_6H_4]_2(^{n}Bu)Sn(SeCH_2CH_2pz)$ (**9**) shows an AB spin system for the same protons. This shows that in solution, at room temperature, the nitrogen atom from the pendant arm of the $2\text{-}(Me_2NCH_2)C_6H_4$ group is involved in an intramolecular interaction with the tin atom (N→Sn) in compound **9**, while for compound **6** only a dynamic behaviour based on decoordination, inversion at nitrogen and re-coordination, as previously described by Iwaoka,[27] can be presumed at room temperature. In the aromatic region, all the compared compounds have one triplet resonance signal and two doublet resonance signals from the pyrazole group.

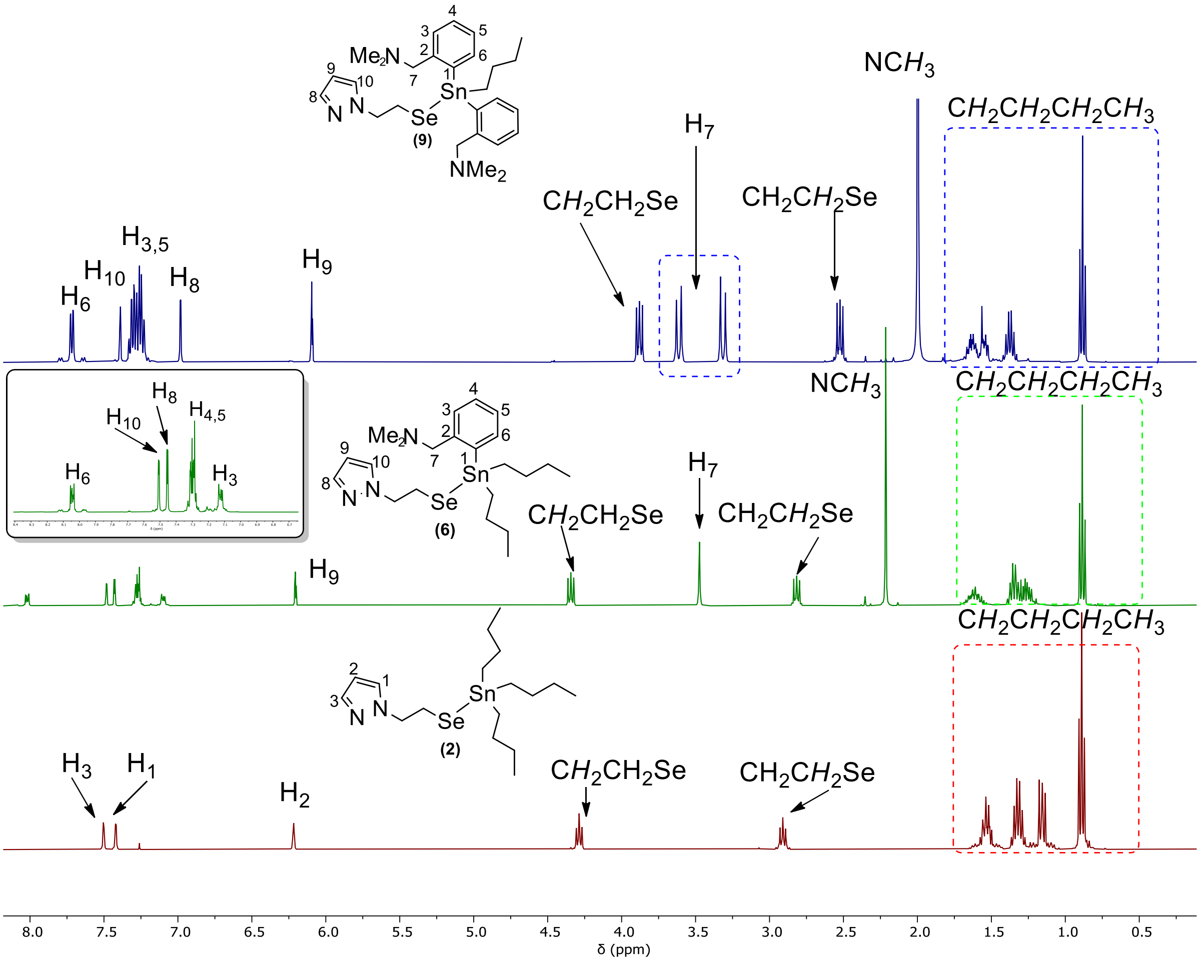

Figure 2. Stacked ^{1}H NMR spectra ($CDCl_3$) of compounds **2**, **6**, and **9**.

The NMR chemical shifts for $^{77}Se\{^{1}H\}$ and $^{119}Sn\{^{1}H\}$ for the discussed compounds and the starting triorganotin(IV) chlorides, as appropriate, are presented in **Table 1**.

Table 1. Centralised NMR data for compounds **1-10** and the triorganotin(IV) chlorides were used as starting materials.

Cpd.	**$^{77}Se\{^{1}H\}$ NMR**			**$^{119}Sn\{^{1}H\}$ NMR**		**Starting material**	**$^{119}Sn\{^{1}H\}$ NMR**
	δ (ppm)	**$^{1}J_{119Sn\text{-}77Se}$ (Hz)**	**$^{1}J_{117Sn\text{-}77Se}$ (Hz)**	**δ (ppm)**	**$^{1}J_{119Sn\text{-}77Se}$ (Hz)**		**δ (ppm)**
1	-193.3	993.7	956.2	60.1	994.2	Me_3SnCl	170.1
2	-228.5	1019.6	971.6	62.3	1018.5	$^{n}Bu_3SnCl$	157.4
3	-227	1170.6	1116.7	-68.7	1172.9	Ph_3SnCl	-45.1
4	-193.9	1209.2	1154.4	4.68	1209.3	Bn_3SnCl	51.1
5	-172.8	822.8	784.3	-59.8	819.8	$R(Me)_2SnCl$	-47.9
6	-218.2	872.9	832.6	-32.9	874.3	$R(^{n}Bu)_2SnCl$	-46.5
7	-69.6	892.3	852.2	-148.4	891.0	$R(Ph)_2SnCl$	-176.3
8	-170.0	814.3	850.7	-107.1	852.1	$R_2(Me)SnCl$	-115
9	-197.1	830.0	874.3	-92.3	872.5	$R_2(^{n}Bu)SnCl$	-114.2
10	-176.7	860.7	901.9	-152.7	902.1	$R_2(Ph)SnCl$	-186.2

The $^{119}Sn\{^{1}H\}$ and $^{77}Se\{^{1}H\}$ NMR spectra display one singlet resonance signal in all compounds, showing the existence of only one tin(IV) species in solution, with a range of 60 ppm to -152 ppm, which are accompanied by selenium satellites with $^{1}J_{119SnSe}$ coupling constants. **Figure 3** presents the $^{77}Se\{^{1}H\}$ and $^{119}Sn\{^{1}H\}$ resonance signals of compound **4**.

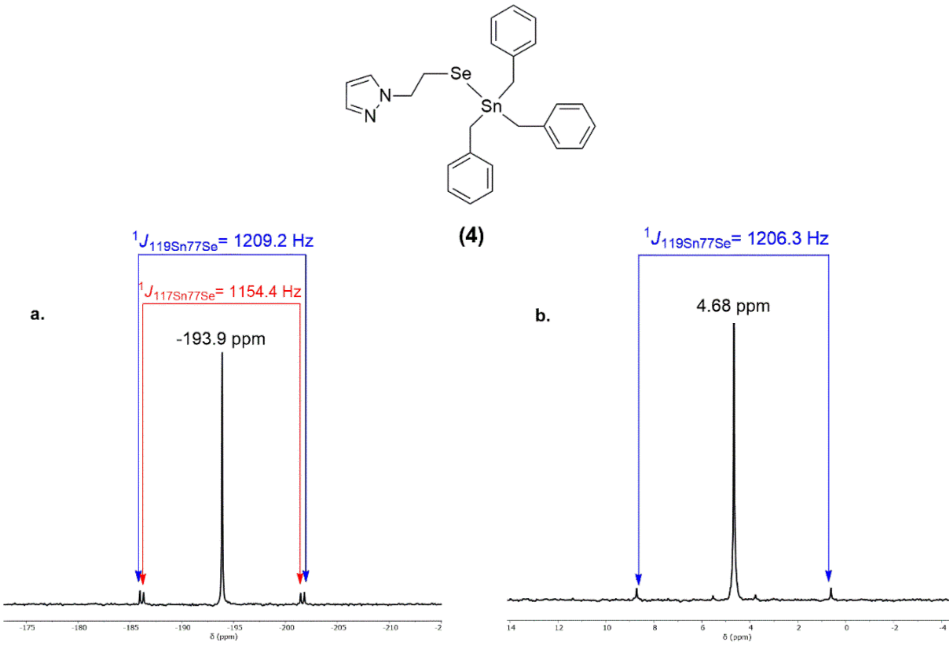

Figure 3. (a) $^{77}Se\{^{1}H\}$ NMR resonance ($CDCl_3$) and (b) $^{119}Sn\{^{1}H\}$ NMR resonance ($CDCl_3$) of compound **4**.

It is precedent in the literature for compounds bearing R_2Sn moieties (R = alkyl) to use the ${}^2J_{119SnH}$ or the ${}^1J_{119SnC}$ coupling constants to assign the coordination geometry about tin in solution, by calculating the values of the C−Sn−C angle.[62-65] These calculations for compounds $R_3Sn(SeCH_2CH_2pz)$ (R = Me, ^{n}Bu, Bn) and $[2-(Me_2NCH_2)C_6H_4](R)_2Sn(SeCH_2CH_2pz)$ (R = Me, ^{n}Bu) are presented in **Table 2**.

Table 2. Values of the calculated C–Sn–C angles in solution and of ${}^2J_{119SnH}$ and ${}^1J_{119SnC}$ coupling constants for compounds **1**, **2**, **4-6**.

Cpd.	**^{1}H NMR**		**^{13}C{^{1}H} NMR**	
	^2J(119Sn,^{1}H)	**C −Sn −C**	**^2J(119Sn,^{13}C)**	**C −Sn −C**
1	59.8	112.0[62]	340.1	106.6[63]
2	-	-	317.5	104.6[63]
4	59.1	111.6[62]	264.7	101.2[64]
5	62.4	113.4[62]	463.6	117.4[63]
6	-	-	450.5	119.7[64]

$\theta = 0.0161|{}^2J|^2 - 1.32|{}^2J| + 133.4$;[62] ${}^1J = 11.4\theta - 875$;[63] ${}^1J = 9.99\theta - 746$;[64]
$\theta = 0.0105|{}^2J|^2 - 0.799|{}^2J| + 122.4$;[62]

These calculations showed that in the homoleptic species, we can assume a monomeric structure with the tin(IV) atom tetrahedrally surrounded by three alkyl groups and a $pzCH_2CH_2Se$ ligand. For the heteroleptic compounds, the results indicate a distorted trigonal bipyramidal geometry, with angles between 117.4° and 119.7°.

The APCI+ and ESI+ mass spectra of the investigated compounds revealed a similar behaviour. The APCI+ HRMS spectrum in methanol of compounds $Bn_3Sn(SeCH_2CH_2pz)$ (**4**) with the identified peaks at *m/z* values 174.97736 $[pzCH_2CH_2Se]^+$, 210.95842 $[M-SnCH_2(C_6H_5)]^+$ and 393.06653 $[M-pzCH_2CH_2Se]^+$ are presented in **Figure 4**.

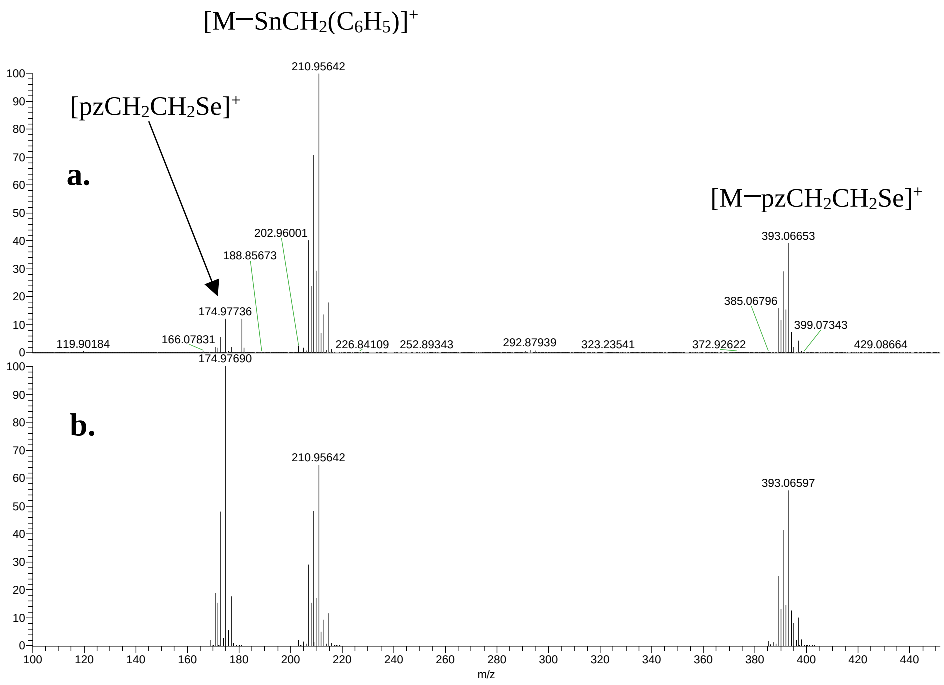

Figure 4. APCI+ HRMS spectrum (in MeOH) of compound **4**: (**a**) experimental and (**b**) simulated.

Single crystals suitable for X-ray diffraction could be grown for compound Ph$_3$Sn(SeCH$_2$CH$_2$pz) (**3**) from a CH$_2$Cl$_2$/hexane system (1:4 v/v), and compound [2-(Me$_2$NCH$_2$)C$_6$H$_4$]$_2$SnSe (**10-a**) by slow evaporation of a CDCl$_3$ solution. The selenium atom in compound **3** is involved in interaction with the tin atom of a neighbour molecule (Se1···Sn1' 3.89 Å vs. Σr_{vdW}(Sn,Se) 4.42 Å[66]), thus resulting in dimeric associations.

The atom numbering scheme and the molecular structure of a dimer in compound **3** are shown in **Figure 5**, and a selection of important interatomic distances and angles is displayed in **Table 3**.

Table 3. Interatomic distances (Å) and angles (°) for compound **3**.

Bond lengths			**Bond angles**	
Sn1−C1	2.1397(1)		C1–Sn1–C7	113.33(1)
Sn1−C7	2.1297(1)		C1–Sn1–C13	110.58(1)
Sn1−C13	2.1423(1)		C7–Sn1–C13	108.08(1)
Sn1–Se1	2.5387(1)		Se1–Sn1–C1	100.82(1)
N2···H19A	2.625(2)		Se1–Sn1–C7	112.48(1)
Se1−Se1'	3.6926(4)		Se1–Sn1–C13	111.49(1)
Sn1−Sn1'	3.5411(4)		Sn1–Se1–C19	97.32(1)
			C1−Sn1−Se1'	161.4(5)

The selenium atom, due to the bridging behaviour becomes tricoordinate, with a coordination geometry in the form of a trigonal pyramid (Sn1–Se1–C19 97.32(1)° and Sn1–Se1–Se1' 119.17(1)°), with the base formed by the Sn1, C19 and Sn1' atoms and Se1 displayed above this plane at a distance of 0.54 Å. The coordination geometry of the tin atom is a distorted trigonal bipyramid (C1−Sn1−Se1' 161.4(5), $\tau = 0.80$),[67] and the tin atom is above the SeC7C14 plane at 0.70 Å. The nitrogen atoms in the planar pyrazole ring have sp^2 hybridization. The lone pair of electrons of N2 in the pyrazole ring is involved in secondary bonding with the H19A proton in the $CH_2C\mathit{H}_2Se$ moiety (N2···H19A 2.625(2) Å, vs. Σr_{vdW}(N,H) 2.86 Å[66]), and in this way, a polymeric chain of dimers is formed (**Figure 6**).

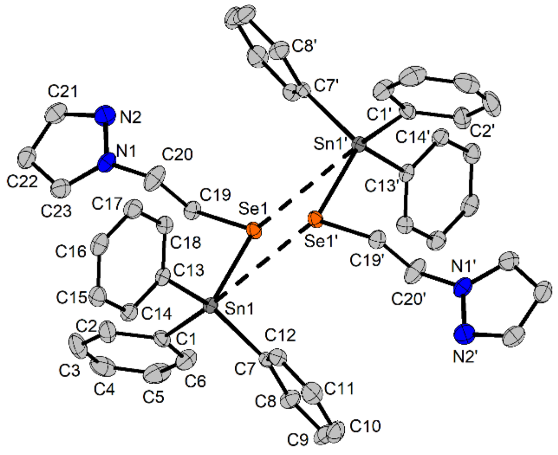

Figure 5. ORTEP-like representation of a dimer in the crystal of compound **3**, with thermal ellipsoids at a 50% probability level. Hydrogen atoms were omitted for clarity. Symmetry equivalent positions (1-x, 1-y, 1-z) are given by "prime"

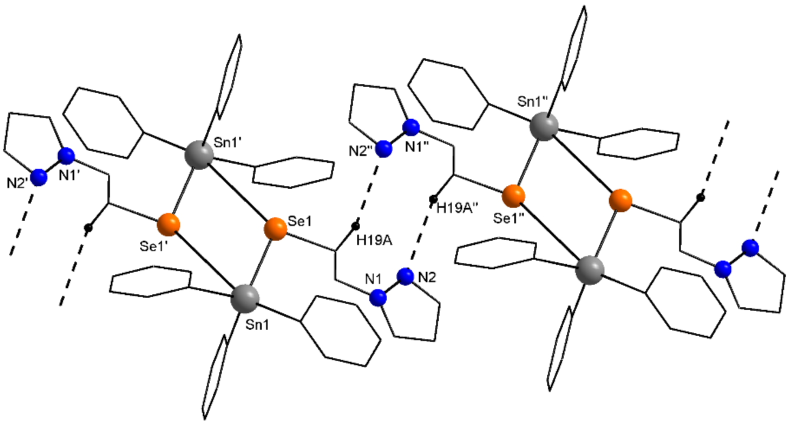

Figure 6. A chain of dimers in the crystal of compound **3**. N2···H19A' 2.625(2) Å. Symmetry equivalent positions (1-x, 1-y, 1-z) and (-x, 1-y, 1-z) are given by "prime" and "double prime", respectively.

A 3D supramolecular network is formed by π CH···Cg short contacts [H3···Cg2(C13-C18) 2.95 Å and H15···Cg1(C1-C6) 2.92 Å]. A view of the 3D network is presented in **Figure 7**.

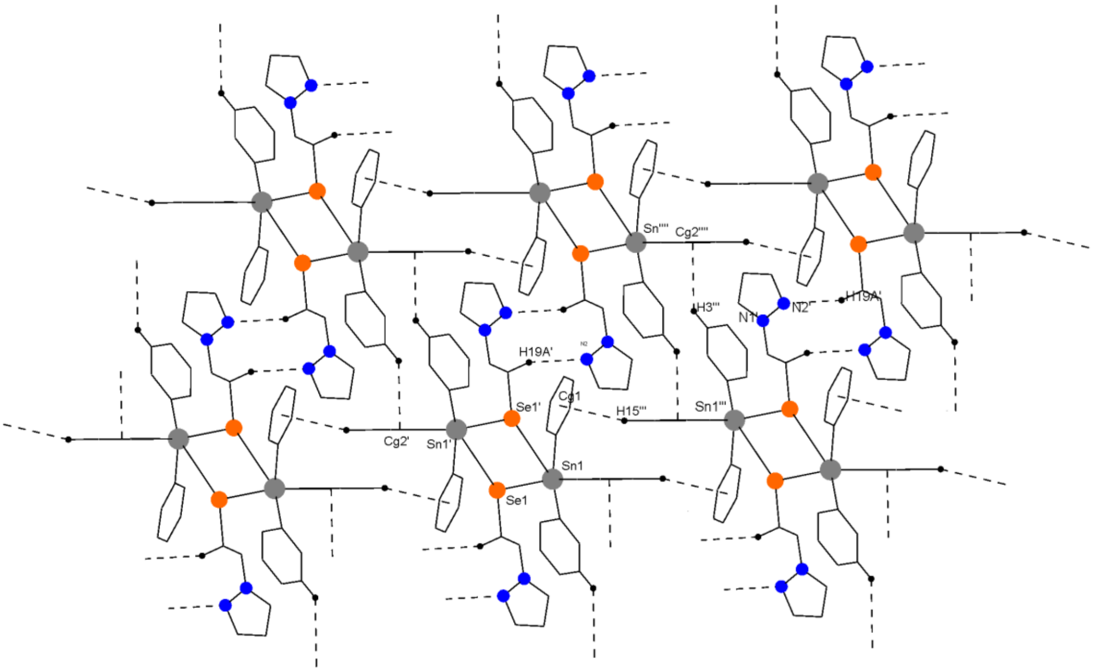

Figure 7. Best view of the supramolecular network in the crystal of compound **3.** Symmetry equivalent positions (1-x, 1-y, 1-z), (-x, 1-y, 1-z), (3/2-x, 1/2+y, 3/2-z) and (1+x, y, z) are given by "prime", "double prime", "triple prime" and "quadruple prime", respectively.

Compound **10**, which was isolated as a colourless solid, decomposed in $CDCl_3$ solution in the NMR tube and formed a microcrystalline precipitate. A single crystal was investigated by X-ray diffraction. The obtained data proved a dimeric structure without the $pzCH_2CH_2Se^-$ ligand, with the formula $\{[2-(Me_2NCH_2)C_6H_4]_2SnSe\}_2$ (**10-a**). The dimeric structure is displayed in **Figure 8,** and important bond lengths and angles are given in **Table 4**.

Table 4. Interatomic distances (Å) and angles (°) for compound **10-a**

Bond lengths			**Bond angles**				
Sn1−Se1	2.5657(2)		Se1−Sn1−Se1'	92.04(1)		C10−Sn1−Se1	108.06(1)
Sn1−Se1'	2.6144(2)		N1−Sn1−Se1	83.98(1)		C10−Sn1−Se1'	105.04(1)
Sn1−N1	2.7100(2)		N1−Sn1−Se1'	171.17(1)		Sn1−Se1−Sn1'	87.96(1)
Sn1−N2	3.049(1)		N1−Sn1−C1	71.24(1)		N2−Sn1−Se1	170.12(3)
Sn1−C1	2.1440(1)		N1−Sn1−C10	83.71(1)		N2−Sn1−Se1'	80.71(3)
Sn1−C10	2.1497(1)		C1−Sn1−Se1	109.20(1)		N2−Sn1−C1	79.15(5)
Se1−Se1'	3.7276(4)		C1−Sn1−Se1'	102.87(1)		N2−Sn1−C10	67.87(5)
Sn1−Sn1'	3.5974(4)		C1−Sn1−C10	131.93(1)		N2−Sn1−N1	104.11(4)

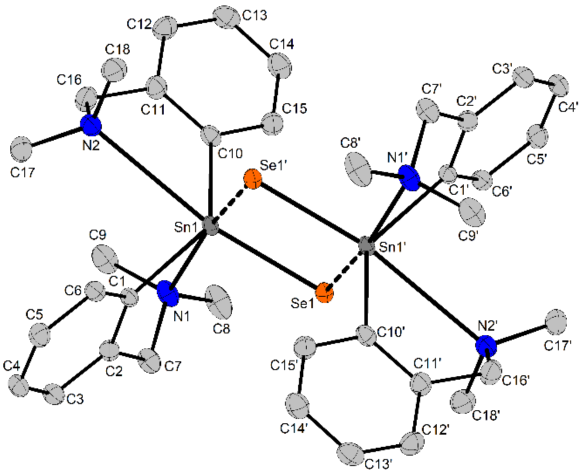

Figure 8. ORTEP-like representation of compound **10-a**, with thermal ellipsoids at 50% probability level. Hydrogen atoms were omitted for clarity. Symmetry equivalent positions (1-x, 1-y, 1-z) are given by “prime”.

The tin atoms have a distorted octahedral coordination geometry, while the selenium atoms have an angular coordination environment [Sn1−Se1−Sn1' 87.96(1)°]. The pendant arms of the 2-(Me$_2$NCH$_2$)C$_6$H$_4$ groups are intramolecularly coordinated to tin, thus inducing planar chirality, with the C$_6$H$_4$ rings as chiral planes and nitrogen as pilot atoms. In this way, R_N and S_N isomers are present in the crystal, with respect to both N1 and N2 atoms. Moreover, the tin atoms themselves are chiral, thus determining Δ_{Sn} and Λ_{Sn} isomerism for this compound as well.[68] In this way, each dimer in the crystal is formed by $\Delta_{Sn1}S_{N1}S_{N2}$ and $\Lambda_{Sn1'}R_{N1'}R_{N2'}$ isomers. The two N→Sn intramolecular and the Se→Sn intermolecular interactions determine the formation of a *12−Sn−6* hypercoordinate species.[69] A chain-like supramolecular association of dimers (**Figure 9**) is formed by π Cg···Cg and π CH···Cg interactions. The Cg2 ring is involved both in Cg···Cg interactions with the Cg2 ring in a neighbour dimer (Cg2···Cg2 3.81 Å, α = 0°, β = 25.6°), and as well with a CH proton of the C$_6$H$_4$ ring with the centroid Cg1 of the neighbour dimer (H12···Cg1 2.74 Å, γ = 10°, C12−H12···Cg1 151°).

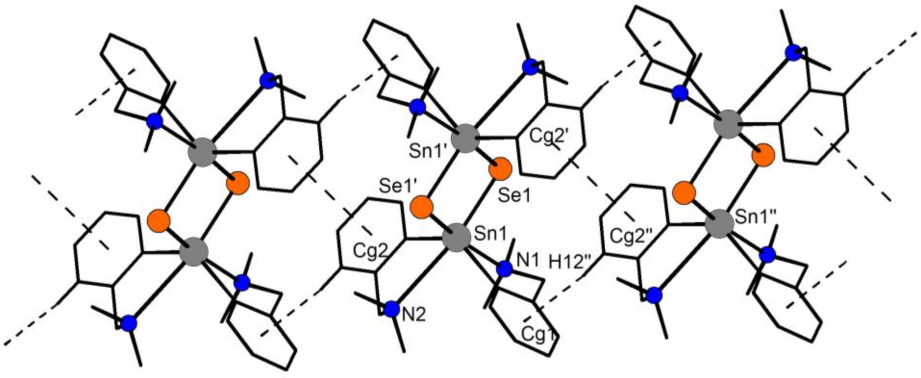

Figure 9. A chain in the crystal of **10-a**. Hydrogen atoms were omitted for clarity. Symmetry equivalent positions (1-x, 1-y, 1-z) and (-x, 1-y, -z) are given by "prime" and "double prime", respectively.

3.1.2. Conclusions

Four homoleptic triorganotin(IV) compounds of type $R_3Sn(SeCH_2CH_2pz)$ [R = Me (**1**), ^{n}Bu (**2**), Ph (**3**), Bn (**4**)] and six heteroleptic triorganotin(IV) complexes with organoselenolato ligands, of type $[2\text{-}(Me_2NCH_2)C_6H_4](R)_2Sn(SeCH_2CH_2pz)$ [R = Me (**5**), ^{n}Bu (**6**), Ph (**7**)] and $[2\text{-}(Me_2NCH_2)C_6H_4]_2(R)Sn(SeCH_2CH_2pz)$ [R = Me (**8**), ^{n}Bu (**9**), Ph (**10**)] were synthesised and characterized using appropriate spectroscopic methods.

The multinuclear ^{1}H and ^{13}C{^{1}H} NMR spectroscopy revealed the expected resonances for all the studied compounds. For compounds $[2\text{-}(Me_2NCH_2)C_6H_4]_2(^{n}Bu)Sn(SeCH_2CH_2pz)$ (**9**)**,** the proton NMR spectrum recorded at room temperature showed an AB spin system for the CH_2NMe_2 protons, thus suggesting that in solution, the nitrogen atom from the pendant arm is involved in an intramolecular interaction. The presence of Se−Sn bonds in solution was ascertained for all compounds through their ^{77}Se and ^{119}Sn NMR spectra, which show ^{77}Se-^{119}Sn and $^{117/119}$Sn-^{77}Se couplings.

Based on the $^{2}J_{SnH}$ and the $^{1}J_{SnC}$ coupling constants in the NMR spectra, the C−Sn−C angles for compounds **1**, **2**, and **4** were calculated. It was assigned a monomeric structure in solution with a tetrahedral coordination geometry around the tin atom, and for **5** and **6,** a distorted trigonal bipyramidal geometry around the tin atom.

The APCI+ and ESI+ mass spectra revealed the formation of the desired compounds.

For $Ph_3Sn(SeCH_2CH_2pz)$ (**3**), the single crystal X-ray diffraction studies revealed a distorted trigonal bipyramid coordination geometry about tin, due to the formation of dimeric associations through bridging selenium atoms;

Compound **10** decomposed in solution with the formation of the dimeric species $[\{2\text{-}(Me_2NCH_2)C_6H_4\}_2SnSe]_2$ (**10-a**), for which the single crystal X-ray diffraction studies showed a hypercoordinate $12-Sn-6$ species, with a distorted octahedron around each tin atom;

3.2. Diorganotin(IV) organoselenolates

3.2.1. Synthesis and characterisation

The synthesis method is similar to the case of the triorganotin(IV) organoselenolates. After splitting the Se−Se bond in degassed absolute ethanol, under argon, with $NaBH_4$, the resulting sodium organoselenolates were reacted in a 2:1 molar ratio with the corresponding heteroleptic diorganotin(IV) dichloride, as depicted in **Scheme 3,** to obtain complexes **11**, **12**, and **13**. As well, the $[2\text{-}(Me_2NCH_2)C_6H_4](^n Bu)SnCl(SeCH_2CH_2pz)$ **14** was synthesised by reacting the sodium organoselenolate with $[2\text{-}(Me_2NCH_2)C_6H_4](^n Bu)SnCl_2$ in a 1:1 molar ratio. In the same scheme is presented the synthesis of the diorganotin(IV)pseudohalido organoselenolates, where the corresponding diorganotin(IV) bis(pseudohalides) were reacted with the resulting sodium organoselenolates in a 1:1 molar ratio to obtain complexes **16-18**.

Compound $[2\text{-}(Me_2NCH_2)C_6H_4](Me)Sn(NCS)_2$ (**15**) was obtained during the present studies, from the reaction between $[2\text{-}(Me_2NCH_2)C_6H_4](Me)SnCl_2$ and K(SCN) in a 1:2 molar ratio, and it was used further as starting material to obtain complex **16**. A purification process with column chromatography using ethyl acetate and dichloromethane was employed to purify compounds $[2\text{-}(Me_2NCH_2)C_6H_4](^n Bu)Sn(NCS)(SeCH_2CH_2pz)$ (**17**) and $[2\text{-}(Me_2NCH_2)C_6H_4](Ph)Sn(NCS)(SeCH_2CH_2pz)$ (**18**).

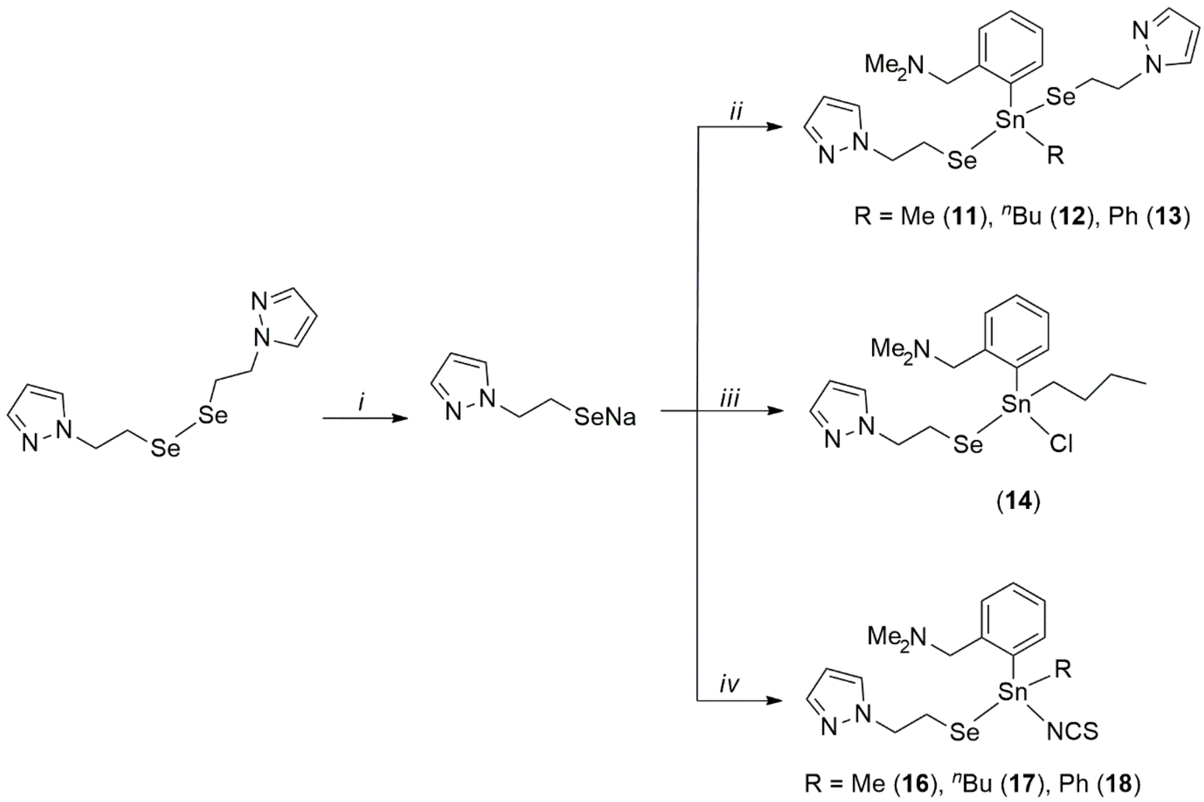

Scheme 3. Synthesis of complexes **11-18**. Reagents and conditions: *i)* $NaBH_4$, degassed absolute ethanol, at 0 °C *ii)* [2-(Me_2NCH_2)C_6H_4](R)$SnCl_2$ (R = Me, ^{n}Bu, Ph), *iii)* [2-(Me_2NCH_2)C_6H_4](^{n}Bu)$SnCl_2$ *iv)* [2-(Me_2NCH_2)C_6H_4](R)Sn$(NCS)_2$ (R = Me, ^{n}Bu, Ph).

Multinuclear NMR (^{1}H, ^{13}C{^{1}H}, ^{77}Se{^{1}H}, ^{19}Sn{^{1}H}) experiments, in $CDCl_3$ solutions, were performed for all compounds. The obtained resonances in the proton and carbon NMR spectra were identified by 2D NMR (H,H-COSY, H,C-HSQC and H,C-HMBC).

Figure 10 presents the ^{1}H NMR spectra of compounds [2-(Me_2NCH_2)C_6H_4](Me)Sn$(SeCH_2CH_2pz)_2$ (**11**), [2-(Me_2NCH_2)C_6H_4](Me)Sn$(NCS)_2$ (**15**) and [2-(Me_2NCH_2)C_6H_4](Me)Sn(NCS)($SeCH_2CH_2pz$) (**16**), which show all the resonance signals expected for the organic groups attached to selenium and tin, respectively. In the case of compounds **11** and **15**, in the aliphatic region, all the expected resonance signals are well-defined. For these complexes, we can see one sharp singlet resonance signal corresponding to the methyl group bound to the tin atom; the signal with the chemical shift value 0.96 ppm (**11**) is accompanied by tin satellites, with $^2J_{117SnH}$ 63.2 Hz and $^2J_{119SnH}$ 66.5 Hz coupling constants, while the signal with a chemical shift value of 1.12 ppm in the spectrum of **15** is accompanied by tin satellites with $^2J_{117SnH}$ 78.7 Hz and $^2J_{119SnH}$ 82.2 Hz coupling constants. Last but not least, the value of 1.01 ppm in the spectrum of **16** is accompanied by tin satellites with $^2J_{117SnH}$ 71.3 Hz and $^2J_{119SnH}$ 74.6 Hz.

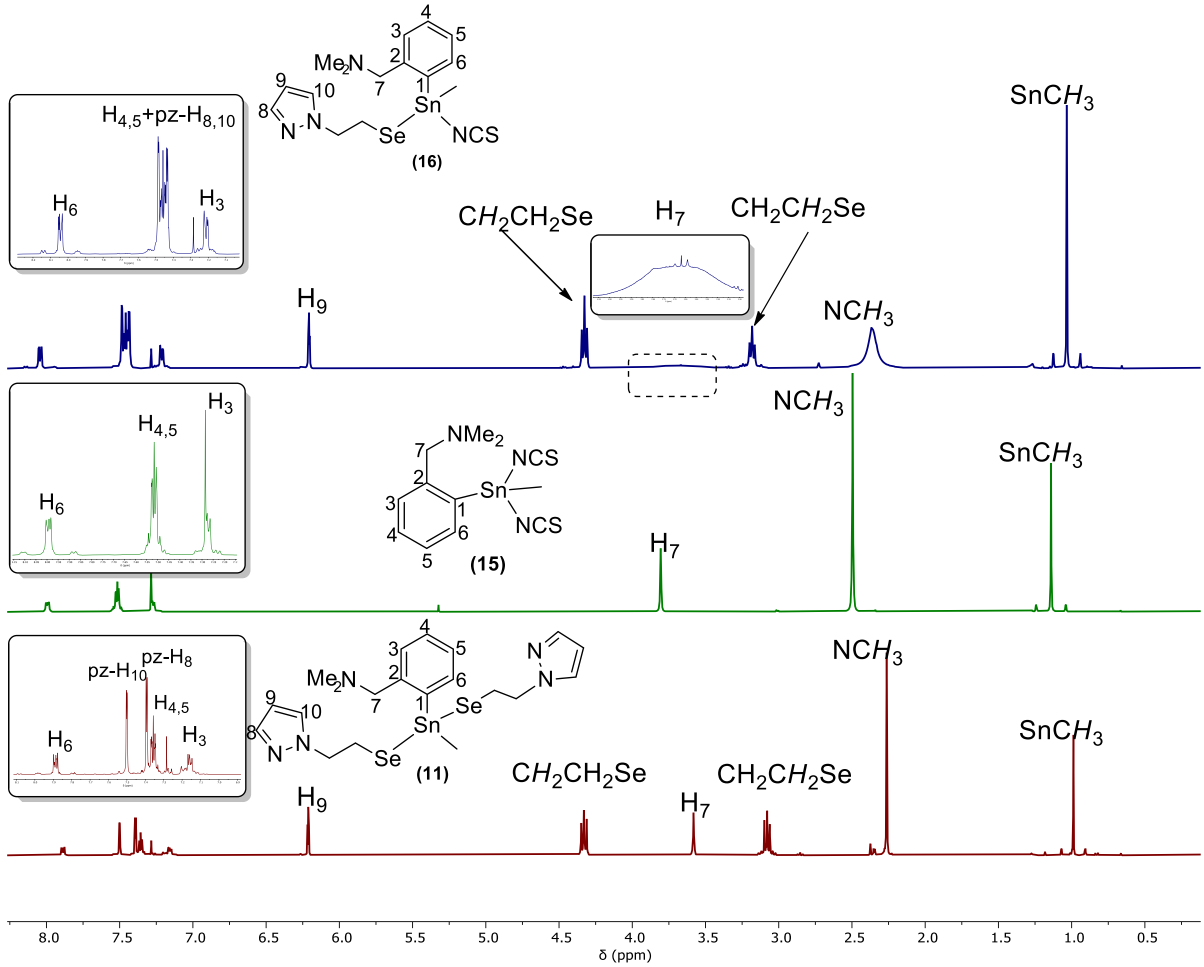

Figure 10. ^{1}H NMR spectra (CDCl$_3$) of compounds [2-(Me$_2$NCH$_2$)C$_6$H$_4$](Me)Sn(SeCH$_2$CH$_2$pz)$_2$ (**11**) [2-(Me$_2$NCH$_2$)C$_6$H$_4$](Me)Sn(NCS)$_2$ (**15**) and [2-(Me$_2$NCH$_2$)C$_6$H$_4$](Me)Sn(NCS)(SeCH$_2$CH$_2$pz) (**16**).

In the case of compound **16,** in contrast to the other two compounds (where all the singlet resonance signals are sharp), the typical signals for the pendant arm with a chemical shift value of 2.34 ppm and 3.66 ppm are broad and not well-defined at room temperature. This behaviour might be determined by the dynamic process in which the nitrogen atom from the pendant arm is involved in coordination to and decordination from tin, too fast to be captured at the NMR time scale, as was observed previously by Iwaoka.[73]

To prove this theory, the compounds were also measured at variable temperatures; the results are presented in **Figure 11**. The change of the broad singlet resonance signals into an AB spin system at -30˚C/-40˚C can be seen, which means that at low temperature the CH_2N protons and the $N(CH_3)_2$ groups, respectively, are no more equivalent (at -30 °C $\delta(^1H)_{Me}$= 2.24 and 2.46 ppm, and $\delta_A(^1H)_{CH2}$= 3.47 and $\delta_B(^1H)_{CH2}$= 3.94 ppm). A free enthalpy $\Delta G^{\#}$= 58.7

KJ/mol, also were calculated at the coalescence temperature T_c= 15 °C, for the dynamic process suffered by the CH_2 protons in the $CH_2N(CH_3)_2$ pendant arm, and a $\Delta G^{\#}$= 70.8 KJ/mol at T_c= 10 °C for the two methyl groups. Also, the not well resolved multiplet resonance signal from the methylene group in the $SeCH_2CH_2pz$ appears as a double multiplet signal, probably because of the not equivalent hydrogen atoms in the two methylene groups.

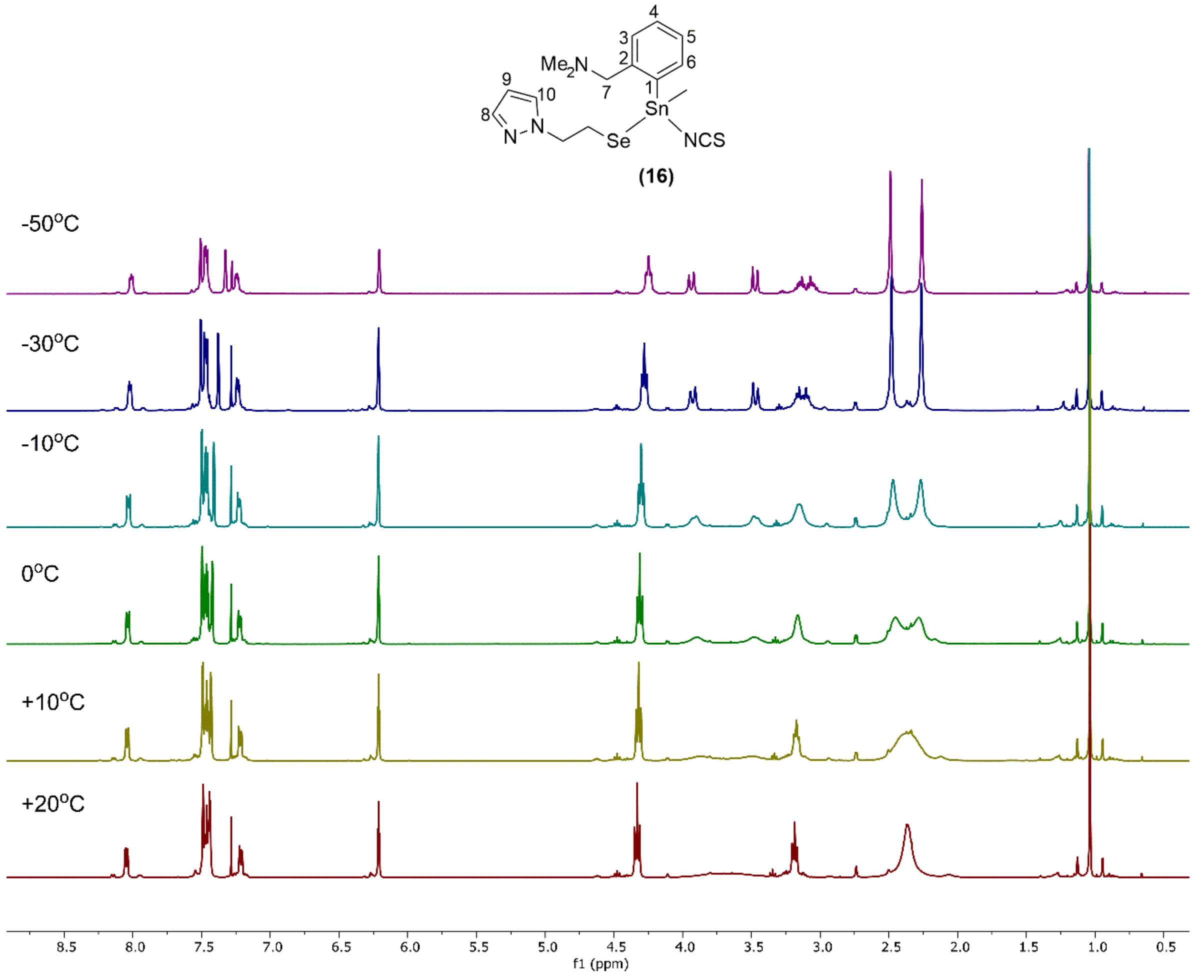

Figure 11. VT ^1H NMR spectra of compound **16** in $CDCl_3$.

In these types of compounds, the presence of the 2-$(Me_2NCH_2)C_6H_4$ group can lead to an increase in the coordination number at the tin atom because of an intramolecular N→Sn coordination. That kind of secondary interaction can be observed in the ^1H and the ^{13}C NMR spectra recorded at room temperature in the case of compound **14**, where the protons from the CH_2 group and the two methyl groups in the $CH_2N(CH_3)_2$ pendant arm are no longer equivalent. The resonance for the CH_2 protons appears as an AB spin system, while the two methyl groups give two singlet resonance signals.

Table 5. NMR data ($CDCl_3$) for compounds **11-18** and their starting materials.

	$^{77}Se\{^1H\}$ NMR			$^{119}Sn\{^1H\}$ NMR		Starting material	$^{119}Sn\{^1H\}$ NMR
	δ (ppm)	$^1J_{119Sn-77Se}$ (Hz)	$^1J_{117Sn-77Se}$ (Hz)	δ (ppm)	$^1J_{119Sn-77Se}$ (Hz)		δ (ppm)
11	-163.6	1117.5	1066.3	-74.2	1116.4	R(Me)$SnCl_2$	-97.3
12	-183.2	1375.5	1317.4	-52.2	1145.2	R(^{n}Bu)$SnCl_2$	-103
13	-182.4	1173.4	1121.7	-107.2	1171.5	R(Ph)$SnCl_2$	-170
14	-160.9	1374.2	1317.4	-104.6	1374.7	R(^{n}Bu)$SnCl_2$	-103
15	-	-	-	-252.7	-	R(Me)$SnCl_2$	-97.3
16	-167.1	1422.3	1353.7	-161.8	1427.1	R(Me)Sn$(SCN)_2$	-252.7
17	-183.2	1145.1	1093.6	-52.2	1151.8	R(^{n}Bu)Sn$(SCN)_2$	-266.6
18	-180.2	1201.2	1112.7	-110.1	1199.5	R(Ph)Sn$(SCN)_2$	-245.3

R = $[2-(Me_2NCH_2)C_6H_4]$

In the case of compound $[2-(Me_2NCH_2)C_6H_4](Me)Sn(NCS)(SeCH_2CH_2pz)$ **(16)**, the $^{119}Sn\{^1H\}$ spectrum shows a different pattern. The observed splitting indicates dipolar interactions involving the two ^{15}N nuclei as well as the ^{119}Sn-^{15}N spin-spin coupling, as outlined by Wrackmeyer.[74] The rest of the $^{119}Sn\{^1H\}$ NMR spectra display one sharp singlet resonance signal for all compounds, showing the appearance of only one species in solution, with a range of -52.2 ppm to -161.8 ppm. The ESI+ mass spectrum of compound **16** displays a single peak at the m/z value of 441.99928, with the expected pattern determined by the isotopic composition, corresponding to the cation $[M-NCS]^+$ (**Figure 12**). In these types of compounds, a similar behaviour can be observed when, upon ionization, the tested compounds lose the $[M-SCN]^+$ fragment.

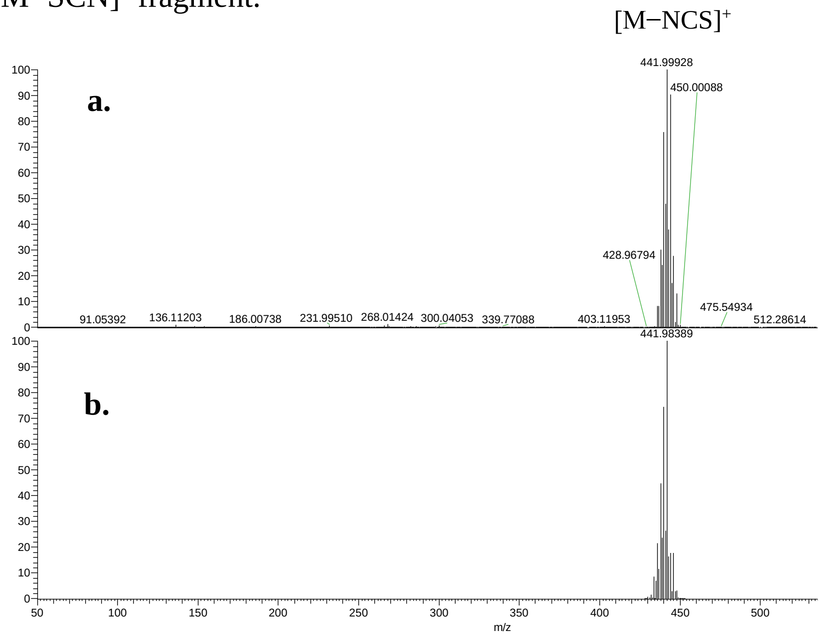

Figure 12. Experimental (a) and calculated (b) ESI+ MS spectra (in MeOH) of compound **16**.

The effort to obtain single crystals of compound **11** led to its decomposition in solution, resulting in the formation of a solid product with a dimeric structure, identified as {[2-(Me_2NCH_2)C_6H_4](Me)SnSe}$_2$ (**11-a**) (**Figure 13**). The same situation happened to compound **12**. After slow evaporation of the $CDCl_3$ solution from the NMR tube, a solid microcrystalline product formed, and it was investigated by X-ray diffraction when a dimeric species of type {[2-(Me_2NCH_2)C_6H_4](^{n}Bu)SnSe}$_2$ (**12-a**) (**Figure 14**) was found.

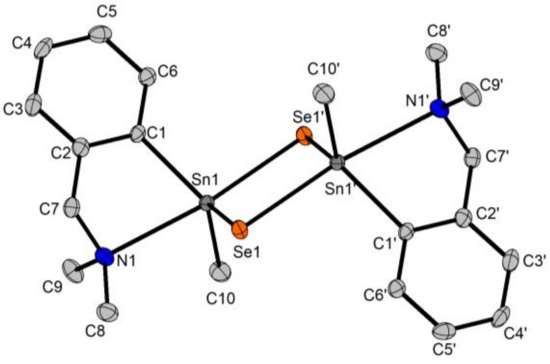

Figure 13. Thermal ellipsoids representation of a dimeric unit in compound **11-a**. Hydrogen atoms were omitted for clarity. Symmetry equivalent positions (-x, 1-y, -z) are given by "prime".

All the important interatomic distances and bond angles for compounds **11-a** and **12-a** are given in **Table 6**.

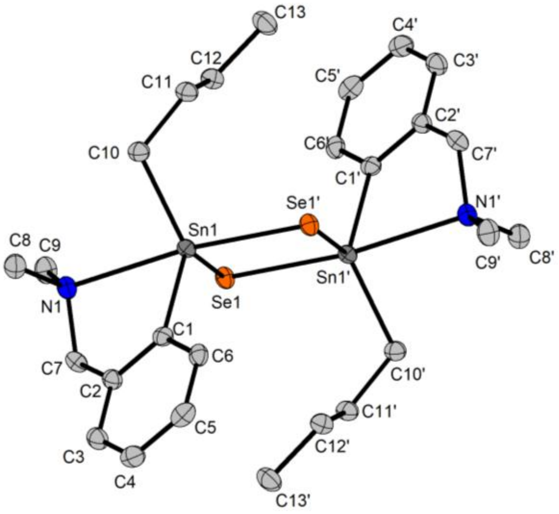

Figure 14. Thermal ellipsoids representation of a dimeric unit in compound **12-a**. Hydrogen atoms were omitted for clarity. Symmetry equivalent positions (1-x, 1-y, 1-z) are given by "prime".

Table 6. Important interatomic distances and bond angles in **11-a** and **12-a.**

Bond / Angle	**11-a**	**12-a**
Sn1−Se1	2.5033(3)	2.5317(2)
Sn1−Se1'	2.6545(3)	2.6475(4)
Sn1−N1	2.5633(3)	2.6046(2)
Sn1−C1	2.1434(2)	2.1528(1)
Sn1−C10	2.1365(2)	2.1662(1)
Se1−Se1'	3.7960(4)	3.8025(5)
Sn1−Sn1'	3.4952(4)	3.5183(4)
Se1−Sn1−Se1'	94.73(1)	94.45(1)
N1−Sn1−Se1	88.60(1)	87.11(1)
N1−Sn1−Se1'	173.16(1)	172.01(6)
N1−Sn1−C1	73.83(1)	72.89(1)
N1−Sn1−C10	85.76(1)	84.82(1)
C1−Sn1−Se1	114.27(1)	111.92(1)
C1−Sn1−Se1'	99.35(1)	99.30(7)
C1−Sn1−C10	124.23(1)	123.22(1)
C10−Sn1−Se1	116.50(1)	118.42(1)
C10−Sn1−Se1'	98.05(1)	101.23(7)
Sn1−Se1−Sn1'	85.27(1)	85.55(1)

Some similarities can be observed in both molecular structures. The molecules form dimeric units through selenium atoms, which are interacting with both tin atoms at nearly identical distances (range 2.5033(3)Å - 2.6545(3) Å, vs. Σr_{cov}(Sn,Se) 2.59 Å and Σr_{vdW}(Sn,Se) 4.24 Å).[66] In both cases, the tin atoms are very close to each other with a Sn···Sn distance of 3.4952(4)Å in **11-a** and 3.5183(4)Å in **12-a**, shorter than the Σr_{vdW}(Sn,Sn) of 4.84 Å.[66] Planar Sn_2Se_2 cores are formed, with Se−Sn−Se angles of 94.73(1)° in **11-a** and 94.45(1)° in **12-a.**

The coordination geometry of the selenium atom is angular, with Sn−Se−Sn angles of 85.27(1)°, in the case of compound **11-a**, and 85.55(1)° in **12-a**. The nitrogen atom from the pendant arm is intramolecularly coordinated to tin, forming a tin(IV) hypercoordinated species in both cases,[69] and the displayed coordination geometry is trigonal bipyramidal (τ_5 = 0.81 for both compounds).[67]

The compounds display planar chirality with a non-planar SnC_3N five membered ring. In that chirality, the nitrogen atom plays a key role and serves as the pilot atom with the C_6H_4 ring as the chiral plane, thus leading to the formation of R_N and S_N isomers.

In the crystal of compound **11-a**, CH···Se contacts just at the limit of the sum of the two elements are present (H5···Se1 3.028 Å, vs. Σr_{vdW}(H,Se) 3.10 Å[66] while in the crystal of compound **12-a**, chains are formed by π HCH···Cg interactions, based on a CH_2 proton in the ^{n}Bu group (H10B···Cg 2.81 Å, γ = 5.8°, C10−H10B···Cg 141°).[75,76] The chain like association in compound **12-a** is displayed in **Figure 15**.

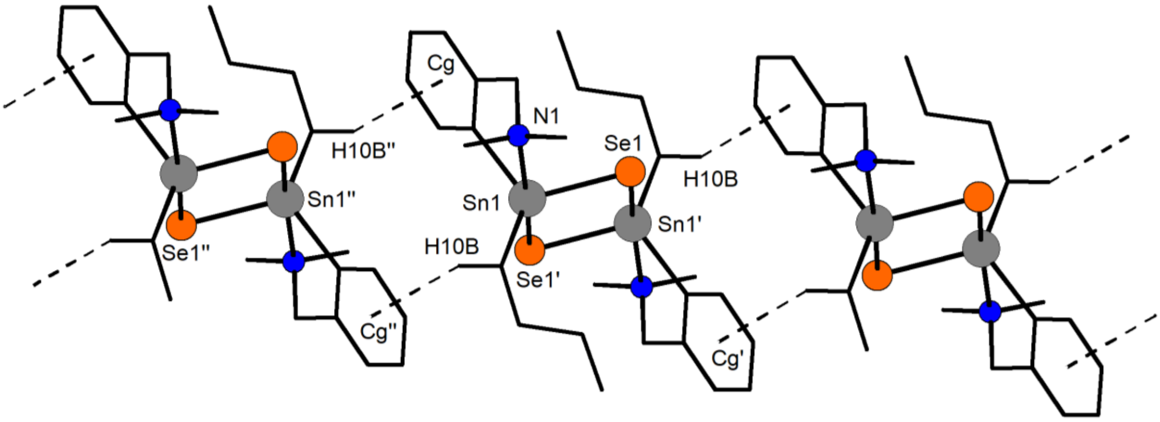

Figure 15. Best view of a chain in the crystal of **12-a**. Hydrogen atoms, except those involved in inter-dimer interactions, were omitted for clarity. Symmetry equivalent positions (-x, 1-y, -z) are given by “prime”.

In the case of compound **12-a**, the chains are formed by π HCH···Cg interactions, based on the a CH_2 proton in the ^{n}Bu group (H10B···Cg 2.81 Å, γ = 5.8°, C10−H10B···Cg 141°).[75,76]

Using slow diffusion within a CH_2Cl_2/n-hexane system (1:4 v/v) as crystallisation method, were obtained single crystals suitable for X-ray diffraction for the complexes [2-$(Me_2NCH_2)C_6H_4$](Me)Sn(SCN)$_2$ (**15**) and [2-$(Me_2NCH_2)C_6H_4$](Me)Sn(SCN)($SeCH_2CH_2$pz) (**16**).

The crystal of compound **15** contains two independent molecules in the unit cell, and their thermal ellipsoids representations (**15a** and **15b**) are displayed in **Figure 16**.

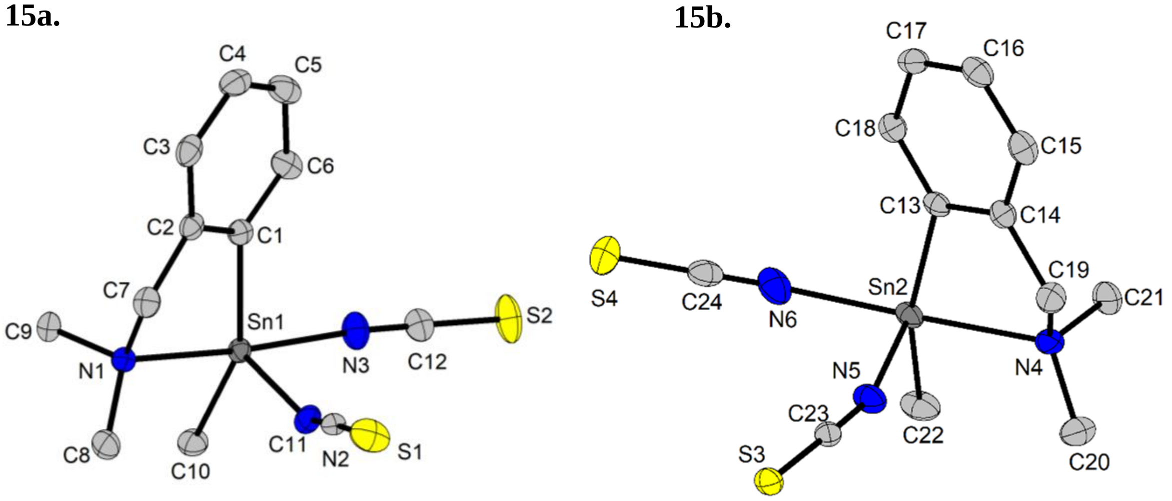
15a. **15b.**

Figure 16. Thermal ellipsoids representation of the two independent molecules in the crystal of compound **15**. Hydrogen atoms were omitted for clarity.

The NCS groups behave as isothiocyanato moieties, with a linear N=C=S structure (angles in the range 177.35(1)°−179.58(1)°), and the 2-$(Me_2NCH_2)C_6H_4$ group behaves as a *C,N*-chelating moiety, thus resulting in a *10−Sn−5* hypercoordinate species.[69]

The coordination geometry is a distorted square pyramid ($\tau_5 = 0.26$ in **15a** and $\tau_5 = 0.16$ in **15b**), with an intramolecular N→Sn coordination. Like this, a non-planar five-membered ring is formed in each molecule, folded about the imaginary Sn···CH_2 axis (Sn1···C7 in **15a** and Sn2···C19 in **15b**).

Therefore, planar chirality is present, which determines that a racemic mixture of R_N and S_N isomers in the crystal.[68] Because the tin atom itself becomes chiral in the structure of **15,** the crystal also contains a racemic mixtures of $A_{Sn1},R_{N1}/C_{Sn1},S_{N1}$ and $C_{Sn2},S_{N4}/A_{Sn2},R_{N4}$ isomers.

A selection of important bond angles and interatomic distances for the two independent molecules in **15**, and for compound **16**, is given in **Table 7**.

Table 7. Important interatomic distances and bond angles in **15a**, **15b**, and **16.**

Bond / Angle	15a		15b	Bond / Angle	16
Sn1−N1	2.3926(1)	Sn2−N4	2.3804(1)	Sn1−Se1	2.5298(3)
Sn1−N2	2.1183(1)	Sn2−N5	2.1567(1)	Sn1−N1	2.4110(3)
Sn1−N3	2.1874(1)	Sn2−N6	2.1848(1)	Sn1−N2	2.2410(2)
Sn1−C1	2.1082(1)	Sn2−C13	2.1178(1)	Sn1−C1	2.1231(2)
Sn1−C10	2.1075(1)	Sn2−C22	2.1051(1)	Sn1−C10	2.1202(2)
N2−C11	1.1460(1)	N5−C23	1.1615(1)	N2−C11	1.1354(1)
N3−C12	1.1605(1)	N6−C24	1.1229(1)	S1−C11	1.6273(2)
S1−C11	1.6094(1)	S3−C23	1.6159(1)		
S2−C12	1.6241(1)	S4−C24	1.6229(1)		
Sn1'−S3	3.2876(6)	Sn2−S2	3.1441(7)		
N1−Sn1−N2	86.74(1)	N4−Sn2−N5	84.37(1)	N1−Sn1−Se1	89.85(1)
N1−Sn1−N3	170.38(1)	N4−Sn2−N6	167.92(1)	C1−Sn1−Se1	114.92(1)
N2−Sn1−N3	88.58(1)	N5−Sn2−N6	87.47(1)	C1−Sn1−C10	127.58(1)
N1−Sn1−C1	77.63(1)	N4−Sn2−C13	76.63(1)	C10−Sn1−Se1	116.46(1)
N1−Sn1−C10	94.07(1)	N4−Sn2−C22	93.64(1)	N2−Sn1−Se1	93.37(1)
C1−Sn1−C10	154.39(1)	C13−Sn2−C22	158.17(1)	N2−Sn1−C1	92.91(1)
N2−Sn1−C1	99.80(1)	N5−Sn2−C13	99.24(1)	N2−Sn1−C10	93.86(1)
N2−Sn1−C10	103.91(1)	N5−Sn2−C22	99.18(1)	N2−Sn1−N1	169.64(1)
N3−Sn1−C1	94.91(1)	N6−Sn2−C13	95.97(1)	N2−C11−S1	179.09(1)

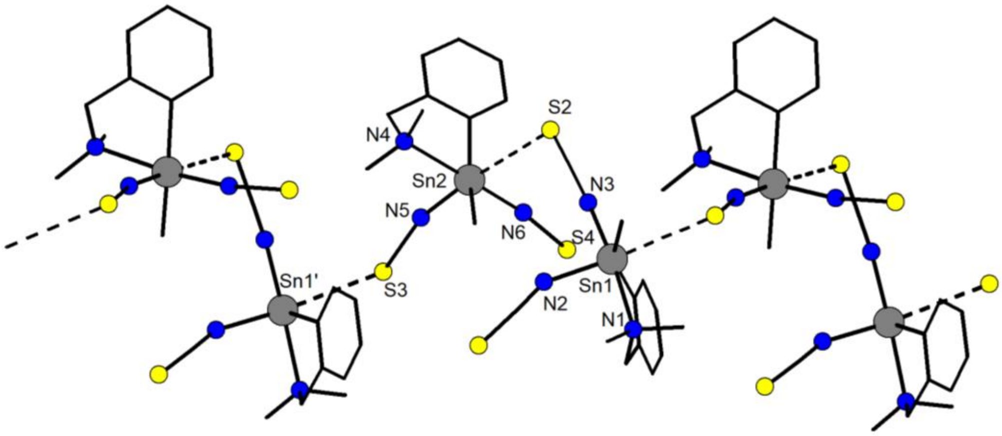

Figure 17. Best view of a chain in the crystal of **15**. Hydrogen atoms, except those involved in inter-dimer interactions, were omitted for clarity. Symmetry equivalent positions (-x, 1-y, -z) are given by "prime".

Figure 17 presents a polymeric chain in the crystal of compound **15**, formed by the bridging tiochianato ligands S3···Sn1 3.2876(6) Å *vs*. Σr_{cov}(Sn,S) 2.44 Å and Σr_{vdW}(Sn,S) 4.31 Å. This interaction modifies the coordination geometry to a distorted octahedron, resulting in a hypercoordinate *12-Sn-6* species. A 3D supramolecular network based on S···H contacts (S4···H21A 2.919 Å, S4···H17 2.717 Å, and S4···H7A 3.008 Å, vs. Σr_{vdW}(S,H) 3.10 Å) is formed (**Figure 18**).

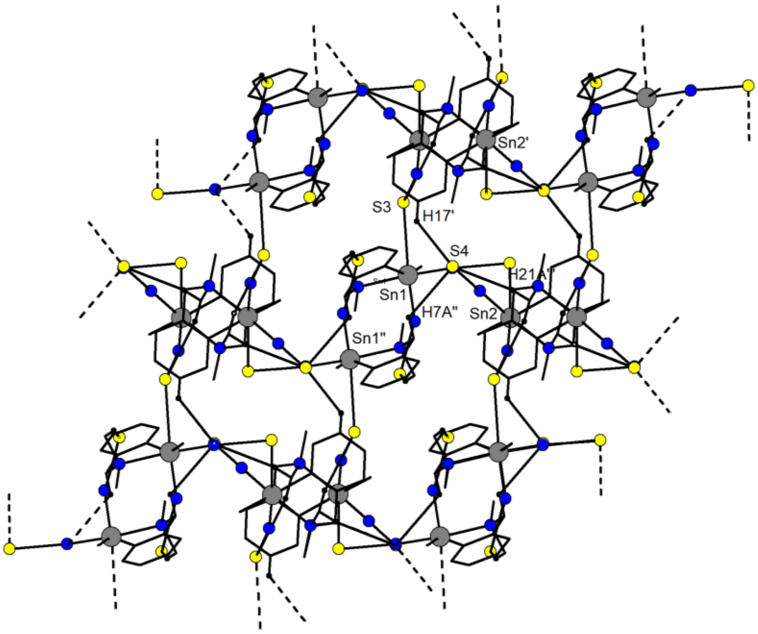

Figure 18. 3D network in the crystal of **15** (view along axis b).

In compound [2-(Me_2NCH_2)C_6H_4](Me)Sn(NCS)($SeCH_2CH_2pz$) (**16**), the organoselenolato $SeCH_2CH_2pz^-$ ligand functions as a *κSe* monodentate entity with a Sn−Se interatomic distance of 2.5298(3) Å, thus determining, together with the other atoms in the coordination sphere of tin, a *10-Sn-5* hypercoordinate species with a distorted trigonal bipyramide coordination geometry (τ_5 = 0.70) (**Figure 19**).[67]

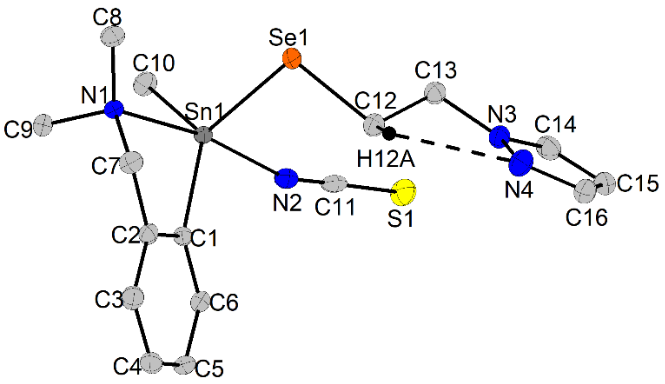

Figure 19. Thermal ellipsoids representation of compound **16**. Hydrogen atoms, except that one involved in intramolecular interaction, were omitted for clarity.

An examination of the crystal structure of this compound revealed π $H_2CH\cdots Cg$ interactions, involving a proton from the tin-bound methyl group, specifically H10C···Cg(C1-C_6) = 3.01 Å (**Figure 20**).

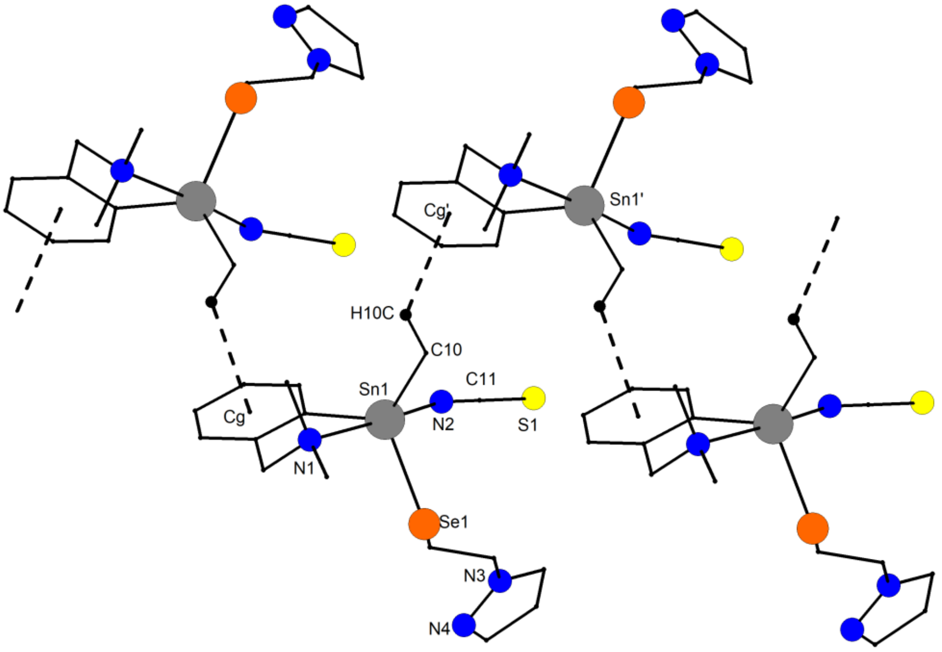

Figure 20. Best view of a chain in the crystal of **16**. Hydrogen atoms, except those involved in intermolecular interactions, were omitted for clarity. Symmetry equivalent positions (1/2+x, y, 1/2-z) are given by “prime”.

3.2.2. Conclusions

Eight diorganotin(IV) compounds with organoselenolato ligands were synthesised and characterised using appropriate methods: three diorganotin(IV) bis(organoselenolates) of type [2-(Me_2NCH_2)C_6H_4](R)Sn($SeCH_2CH_2pz$)$_2$ [R = Me (**11**), ^{n}Bu (**12**), Ph (**13**)], four compounds containing only one organoselenolato ligand, namely $[2\text{-}(Me_2NCH_2)C_6H_4](^n\text{Bu})SnCl(SeCH_2CH_2pz)$ (**14**) and those of type $[2\text{-}(Me_2NCH_2)C_6H_4](R)Sn(NCS)(SeCH_2CH_2pz)$ [R = Me (**16**), ^{n}Bu (**17**), Ph (**18**)], as well as the starting material $[2\text{-}(Me_2NCH_2)C_6H_4](Me)Sn(NCS)_2$ (**15**).

All complexes were characterized by elemental analysis, multinuclear NMR, and mass spectrometry. The ^{1}H NMR spectra of compound **16** showed large resonances for the protons from the alkyl groups in the pendant arm. Variable temperature experiments were performed, when an AB spin system and two singlets were observed for the $CH_2N(CH_3)_2$ protons, respectively.

The APCI+/ESI+ mass spectra showed the base peak with a characteristic pattern, corresponding to the loss of a $SeCH_2CH_2pz$ or an NCS fragment, depending on the composition of the investigated species;

Single crystals of the decomposition products **11-a** and **12-a**, as well as of compounds **15** and **16**, were studied with X-ray diffraction. The N→Sn intramolecular interaction resulted in hypercoordinated species. The studies revealed dimeric structures for $\{[2\text{-}(Me_2NCH_2)C_6H_4](Me)SnSe\}_2$ (**11-a**) and $\{[2\text{-}(Me_2NCH_2)C_6H_4](^n\text{Bu})SnSe\}_2$ (**12-a**) with so much similarity in their structure. The crystal of compound **15** contains two independent molecules in the unit cell, each with a distorted square pyramidal coordination geometry, while the crystal of compound **16** has a distorted trigonal bipyramidal coordination environment about tin.

3.3. Tin(II) organoselenolates

3.3.1. Synthesis and characterisation

After the Se–Se bond in the diorganodiselenide starting material was split with $NaBH_4$, the resulting sodium organoselenolate was reacted in a 1:2 molar ratio with $SnCl_2$ in degassed absolute EtOH to obtain compound **19**. The same procedure, but using a 1:1 molar ratio, was employed in the case of compound **20**. The reaction of **20** with KSCN in a 1:1 molar ratio, in a mixture of solvents ($EtOH/CH_2Cl_2$), led to compound **21** (**Scheme 4**).

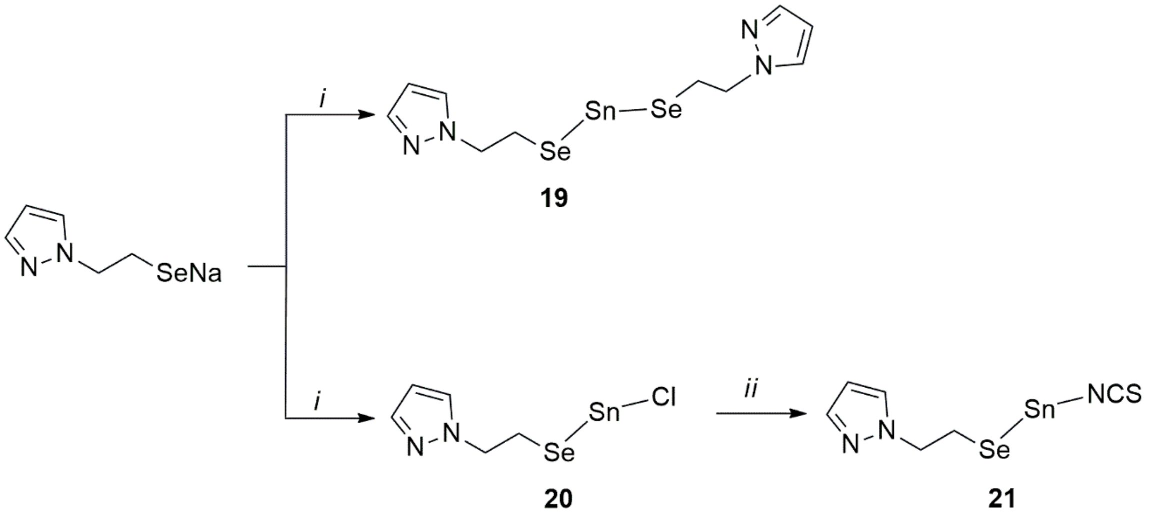

Scheme 4. Synthesis of complexes **19-21**. Reagents and conditions: *i)* $SnCl_2$ in degassed absolute EtOH, *ii)* KSCN in $EtOH/CH_2Cl_2$.

The new compounds were characterised by multinuclear NMR spectroscopy, and the resonance signals were assigned by 2D NMR spectra.

The ^{1}H NMR spectra for the three compounds are presented in **Figure 21**. The spectra revealed the same set of signals with different chemical shift values when compared to the others. In the aliphatic region, the expected multiplet resonances of the CH_2CH_2Se group can be seen, and in the aromatic region, one triplet and two doublet resonance signals from the pyrazole group appear.

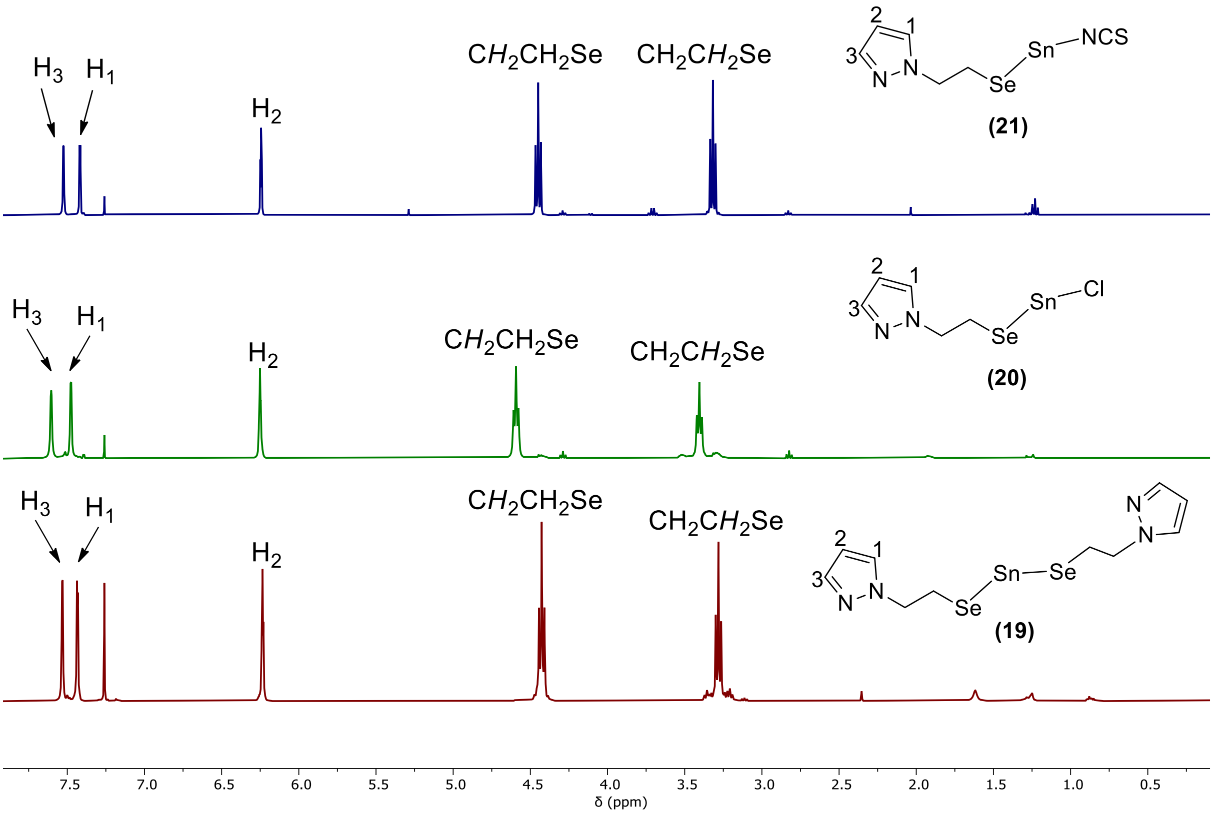

Figure 21. Stacked ^{1}H NMR spectra ($CDCl_3$) of compounds **19-21**.

A similar pattern of resonances can be observed in the carbon NMR spectra for all compounds. The sharp singlet resonance signals for C_5 directly bonded to Se are accompanied by satellites with a coupling constant $^1J_{SnSe}$ of 20.23 Hz (**Figure 22**).

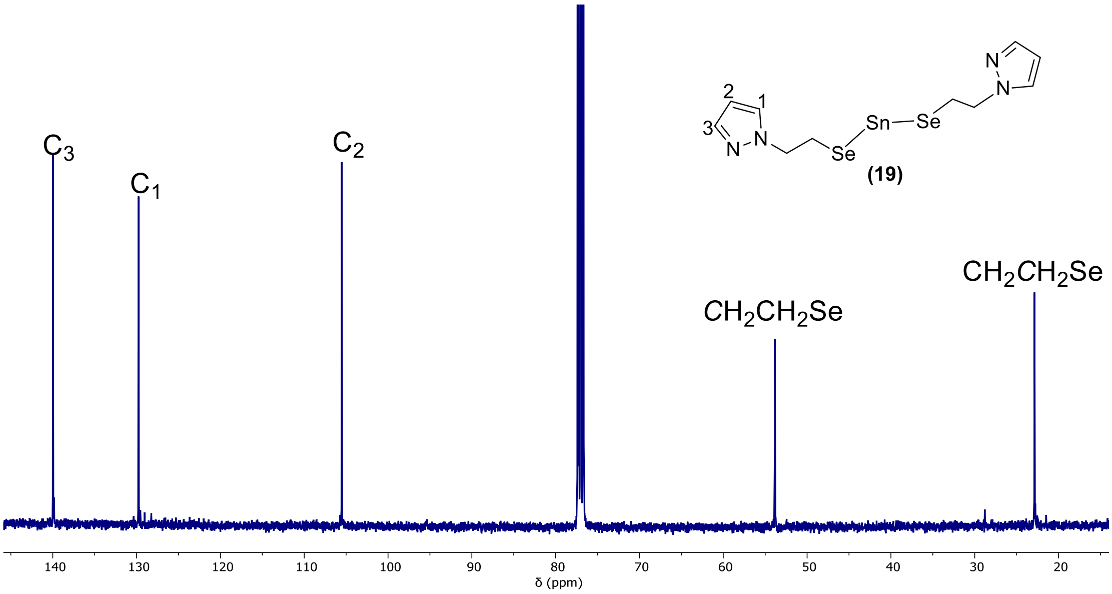

Figure 22. $^{13}C\{^1H\}$ NMR spectra ($CDCl_3$) of compounds **19**.

The $^{77}Se\{^{1}H\}$ and $^{119}Sn\{^{1}H\}$ NMR data for the compounds **19-21** and the starting $SnCl_2$ are presented in **Table 8**.

Table 8. NMR data ($CDCl_3$) for compounds **19-21** and their starting materials.

Cpd.	$^{77}Se\{^{1}H\}$ NMR			$^{119}Sn\{^{1}H\}$ NMR		Starting material	$^{119}Sn\{^{1}H\}$ NMR
	δ (ppm)	$^{1}J_{119Sn-77Se}$ (Hz)	$^{1}J_{117Sn-77Se}$ (Hz)	δ (ppm)	$^{1}J_{119Sn-77Se}$ (Hz)		δ (ppm)
19	-11.5	1513.5	1447.1	-167.6	1511.4	$SnCl_2$	148.9[28]*
20	120.6	1513.5	1447.1	-89.3	-	$SnCl_2$	148.9[28]*
21	291.8	-	-	-109.1	-	**20**	120.6

*benzene-d6

The $^{77}Se\{^{1}H\}$ and the $^{119}Sn\{^{1}H\}$ NMR spectra present one singlet resonance signal for all the presented compounds, and thus undermine the existence of only one species in solution. **Figure 23** presents the observed $^{77}Se\{^{1}H\}$ and $^{119}Sn\{^{1}H\}$ singlet resonances for compound **19**, accompanied by satellites with the corresponding coupling constant, in case of the $^{77}Se\{^{1}H\}$ spectra $^{1}J_{119Sn77Se}$ 1508.94 Hz and $^{1}J_{117Sn77Se}$ 1453.12 Hz, and in case of the $^{119}Sn\{^{1}H\}$ spectra $^{1}J_{77Se119Sn}$ 1516.32 Hz.

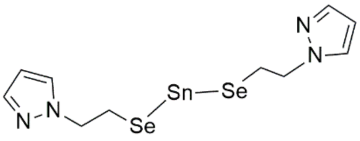

(**19**)

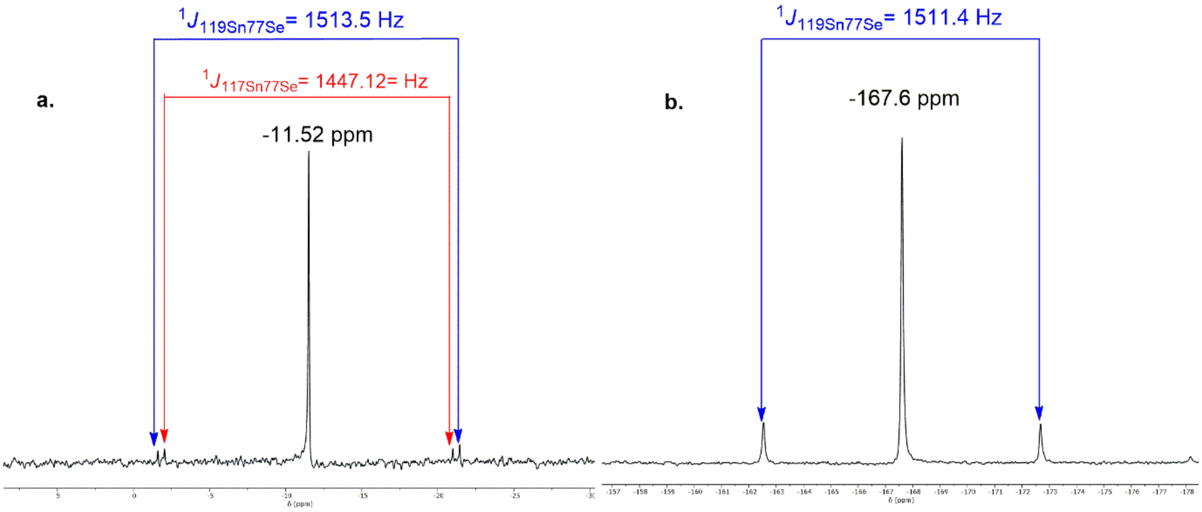

Figure 23. (a) $^{77}Se\{^{1}H\}$ NMR spectrum ($CDCl_3$) and (b) $^{119}Sn\{^{1}H\}$ NMR spectrum ($CDCl_3$) of compound **19**.

The Mass spectrometry, due to the variety of tin and selenium isotopes, is an advantageous characterisation method in this case, also displaying a characteristic pattern for the observed peaks. The peak of the anion $[pzCH_2CH_2Se]^{-}$ was observed in the ESI- MS spectrum of compound **19** at the *m/z* value 174.97685, and it is presented in **Figure 24**.

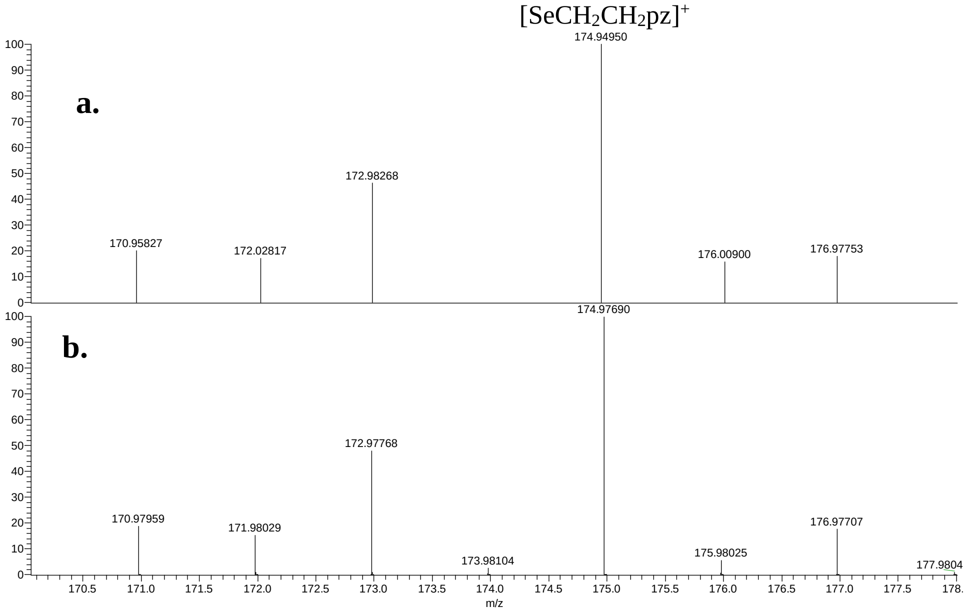

Figure 24. The experimental (**a**) and calculated (**b**) peak of the anionic ligand in the ESI- MS spectrum (in MeOH) of compound **19**.

3.3.2. Conclusions

Three new tin(II) organoselenolates, namely $Sn(SeCH_2CH_2pz)_2$ (**19**) and $SnX(SeCH_2CH_2pz)$ [X = Cl (**20**), NCS (**21**)], were synthesised and characterised.

The ^{1}H and $^{13}C\{^{1}H\}$ NMR spectroscopy have the same set of resonance signals showing the formation of the predicted structure in solution;

The $^{77}Se\{^{1}H\}$ and $^{119}Sn\{^{1}H\}$ NMR spectra display a singlet resonance peak with corresponding coupling constants for all the described compounds, supporting the presence of a single species in solution and the existence of tin-selenium bonds;

The ESI+/APC+ MS spectra of compounds **19-21**, in MeOH solution, showed a peak corresponding to the cation formed by ionisation, after elimination of a $pzCH_2CH_2Se^{-}$, Cl^{-}, or NCS^{-} fragment, respectively.

3.4. Applications

3.4.1. Thermal behaviour

To see the potential of these tin complexes as precursors for tin selenides, we investigated the thermal behaviour of compounds **11, 15, 16** and **19**. The thermal analysis data are displayed in **Figure 25** for **11** and **19**, and in **Figure 26** for **15** and **16**. Compounds **11** (M = 616.12) and **19** (M = 467) were investigated both in inert atmosphere (argon, 100 ml/min) and in synthetic air (100 ml/min, 12 vol.% O_2 in N_2 in the temperature range 25-1000°C. Under a flow of argon, no mass loss was observed until 200°C. In the range 200°C - 346°C, a massive loss of mass was noticed for compound **11**, namely 76.48% (471 g/mol), which suggests the elimination of $Sn(SeCH_2CH_2pz)_2$. The remained quantity of 145 g/mol (23.52%) was unchanged along a plateau until 800°C, and above this temperature, almost all the residue was volatilised.

For the complex $Sn(SeCH_2CH_2pz)_2$ (**19**), we noticed a mass loss of 58.65%, which was assigned to the diorganoselenide $Se(CH_2CH_2pz)_2$. The residue in this case corresponded to SnSe (m = 193 g/mol, 41.35%), a value close to the calculated SnSe content (m = 196, 41.97%) in the starting compound **19**. We presume that the lower mass remaining from compound **11** might be determined by a partial sublimation of this precursor before decomposition, due to its significant volatility.

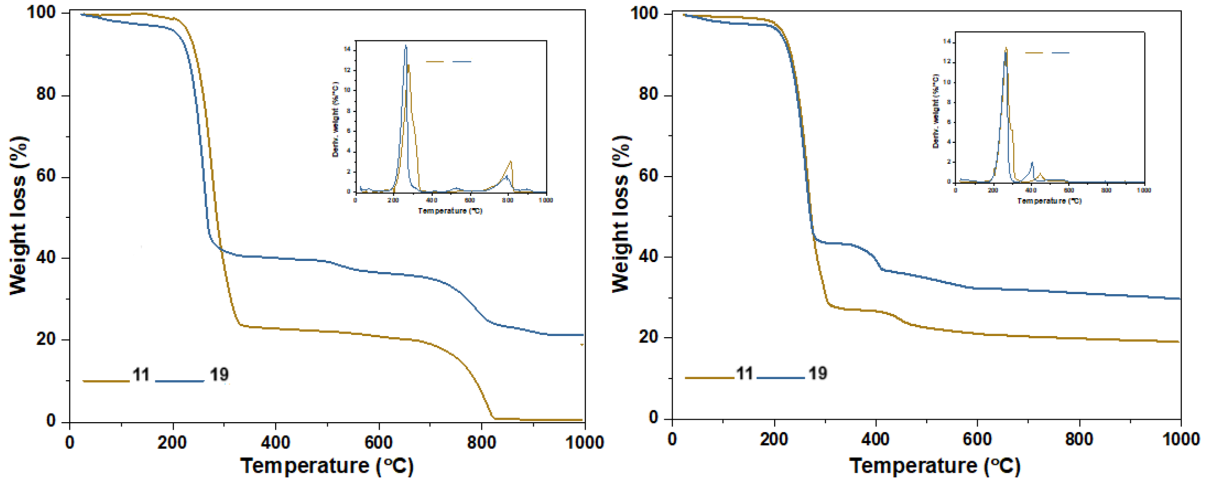

Figure 25. Thermogravimetric analysis data for compounds **11** and **19**, in argon (left), and in synthetic air (right).

The thermogravimetric analyses performed in air for both compounds showed almost the same behaviour in the temperature range 200°C - 400°C, but the weight of the final residue corresponded to metallic tin, e.g. for compound **11,** the remained residue of 19.07% corresponds to a mass of 117 g/mol. For the experiments conducted in synthetic air, we have to consider a more complex pathway, where the formation of oxidized species in the presence of oxygen is expected.

The thermal behaviour of compounds **15** and **16** was investigated only under a flow of synthetic air, when the final residue corresponded, in both cases, to metallic tin. For compound **16** (M = 500.11), in a first degradation step most of the compound was eliminated with a mass loss of 70.74% (m = 355.11 g/mol), which could be assigned formally to $Sn(SeCH_2CH_2pz)(SCN)$ (M = 350.88, calcd. 72.18%), similarly with the situation observed of compound **11**.

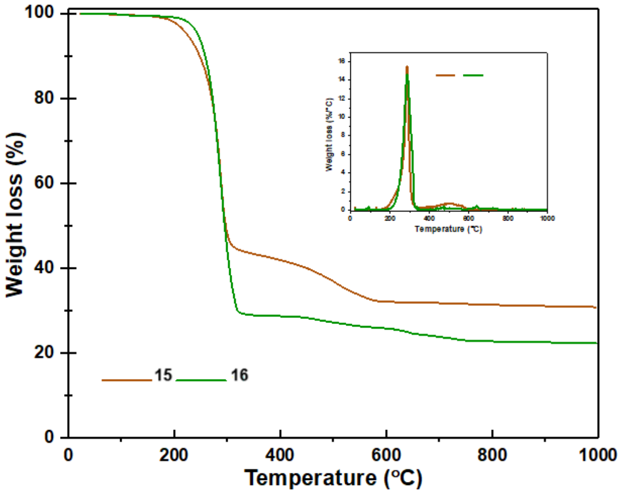

Figure 26. Thermogravimetric analysis data for compounds **15** and **16** in synthetic air.

The resulting data indicate a behaviour closely aligned with that observed in other complexes containing organoselenolato ligands.[79–81] The studied compounds are volatile species, which either sublime before decomposition or decompose easily with the elimination of organoselenium species. Their high volatility recommends them as potential candidates for CVD processes, but the possibility of obtaining tin selenides under certain conditions is not excluded.

3.4.2. Evaluation of the antiproliferative activity

A set of compounds from all the studied classes described in the above subchapters was chosen to evaluate their antiproliferative activity: namely a homoleptic triorganotin(IV) organoselenolate, the complex Ph$_3$Sn(SeCH$_2$CH$_2$pz) (**3**), a heteroleptic triorganotin(IV) organoselenolate, the complex [2-(Me$_2$NCH$_2$)C$_6$H$_4$]$_2$(Ph)Sn(SeCH$_2$CH$_2$pz) (**10**), two diorganotin(IV) compounds, the complexes [2-(Me$_2$NCH$_2$)C$_6$H$_4$](Me)Sn(NCS)$_2$ (**15**), and [2-(Me$_2$NCH$_2$)C$_6$H$_4$](Me)Sn(NCS)(SeCH$_2$CH$_2$pz) (**16**), and two tin(II) organoselenolates, the complexes Sn(SeCH$_2$CH$_2$pz)$_2$ (**19**), and SnCl(SeCH$_2$CH$_2$pz) (**20**).

The antiproliferative activity against the murine melanoma B16.F10 cell line for the tested compounds was performed using the ELISA-BrdU colourimetric assay and various concentrations of the potential active agent. The effect of compounds **3**, **15** and **16** on the cancer cell proliferation is presented in **Figure 27**. **Table 9** displays the IC$_{50}$ values obtained for these compounds, compared with that one observed for the standard drug Dacarbazine. A similar effect can be seen in the case of compounds **10** and **16**, as presented in **Figure 28**.

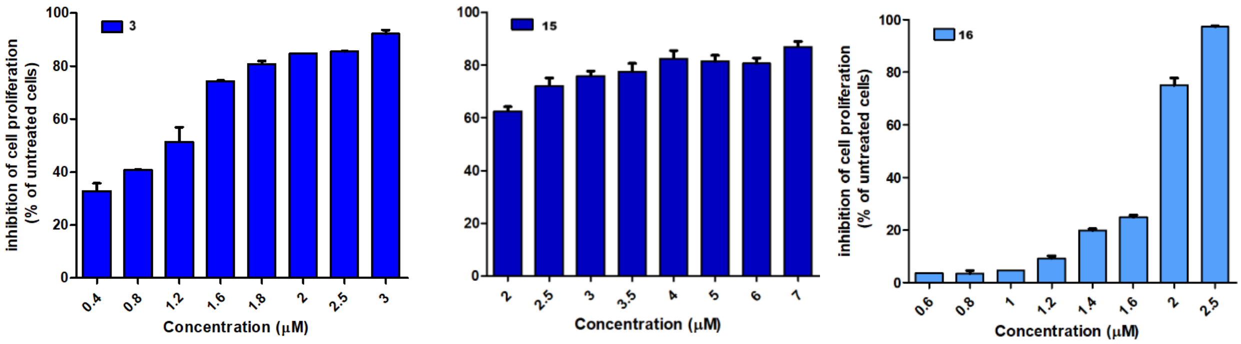

Figure 27. Concentration-dependent antiproliferative effect of compounds **3**, **15** and **16** in comparison with untreated control cells.

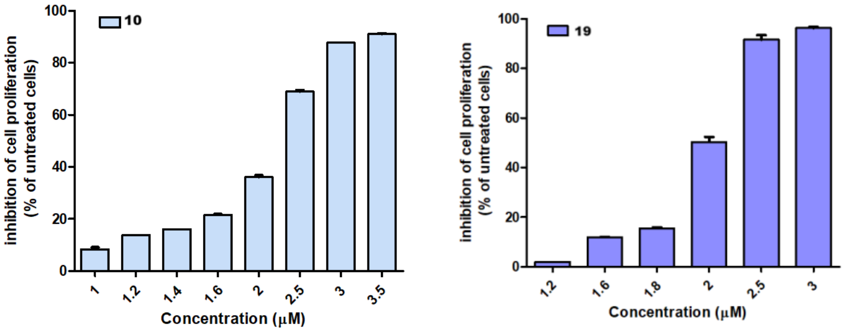

Figure 28. Concentration-dependent antiproliferative effect of compounds **10** and **19** in comparison with untreated control cells.

Table 9. IC_{50} values of the tested compounds.

Compound	**3**	**10**	**15**	**16**	**19**	**20**	Dacarbazine
IC_{50} (μM)	0.86	2.11	3.49	1.76	2.00	8.16	149.7

These results demonstrate an improvement in therapeutic efficacy when compared to the compounds currently employed, e.g. Dacarbazine, Deltonin or Cisplatin in chemotherapy for this specific cell line.[82]

3.4.3. Conclusions

- The thermogravimetric studies for compounds **11**, **15**, **16** and **19** suggested a significant volatility in inert atmosphere, which recommends them as potential candidates for CVD processes;
- The experiments under a flow of synthetic air suggested the possibility of obtaining tin selenides under certain conditions.
- Compounds **3**, **10**, **15**, **16**, **19** and **20** showed a promising antiproliferative activity against the murine melanoma B16.F10 cell line.

5. General conclusions

- Four homoleptic triorganotin(IV) compounds of type $R_3Sn(SeCH_2CH_2pz)$ [R = Me (**1**), ^{n}Bu (**2**), Ph (**3**), Bn (**4**)] and six heteroleptic triorganotin(IV) complexes with organoselenolato ligands, of type $[2\text{-}(Me_2NCH_2)C_6H_4](R)_2Sn(SeCH_2CH_2pz)$ [R = Me (**5**), ^{n}Bu (**6**), Ph (**7**)] and $[2\text{-}(Me_2NCH_2)C_6H_4]_2(R)Sn(SeCH_2CH_2pz)$ [R = Me (**8**), ^{n}Bu (**9**), Ph (**10**)] were synthesised and characterized using appropriate spectroscopic methods.
- Seven diorganotin(IV) compounds with organoselenolato ligands were synthesised and characterized using appropriate methods, i.e. three diorganotin(IV) bis(organoselenolates) of type $[2\text{-}(Me_2NCH_2)C_6H_4](R)Sn(SeCH_2CH_2pz)_2$ [R = Me (**11**), ^{n}Bu (**12**), Ph (**13**)], and four compounds containing only one organoselenolato ligand, namely $[2\text{-}(Me_2NCH_2)C_6H_4](^{n}Bu)SnCl(SeCH_2CH_2pz)$ (**14**) and those of type $[2\text{-}(Me_2NCH_2)C_6H_4](R)Sn(NCS)(SeCH_2CH_2pz)$ [R = Me (**16**), ^{n}Bu (**17**), Ph (**18**)].
- Three new tin(II) complexes, namely $Sn(SeCH_2CH_2pz)_2$ (**19**) and $SnX(SeCH_2CH_2pz)$ [X = Cl (**20**), NCS (**21**)] were synthesised and characterized;
- The starting $[2\text{-}(Me_2NCH_2)C_6H_4](Me)Sn(NCS)_2$ (**15**) was prepared and characterized;
- The multinuclear ^{1}H and $^{13}C\{^{1}H\}$ NMR spectroscopy revealed the expected resonances for all the studied compounds.
- The presence of Se−Sn bonds in solution was ascertained for all compounds through their ^{77}Se and ^{119}Sn NMR spectra, which show $^{77}Se\text{-}^{119}Sn$ and $^{117/119}Sn\text{-}^{77}Se$ couplings.
- Based on the $^{2}J_{SnH}$ and the $^{1}J_{SnC}$ coupling constants in the NMR spectra, were calculated the C−Sn−C angles for compounds **1**, **2**, **4-6**, and for them was assigned a monomeric structure in solution with a tetrahedral coordination geometry around the tin atom.
- Not for all compounds containing the $2\text{-}(Me_2NCH_2)C_6H_4$ group attached to tin could be ascertained a *C*,*N* coordination behaviour in solution. Only for compound 9 the ^{1}H NMR spectrum suggested a N→Sn coordination at room temperature in solution.
- For compound VT ^{1}H NMR spectra were recorded, and at low temperature they were in accordance with the existence of a N→Sn intramolecular interaction.
- The APCI+ / ESI+ mass spectra revealed the formation of the desired compounds;

- For $Ph_3Sn(SeCH_2CH_2pz)$ (**3**), the single crystal X-ray diffraction studies revealed a distorted trigonal bipyramide coordination geometry about tin, based on dimerization by bridging selenium atoms.
- Compounds **10**, **11**, and **12** decomposed in solutions of chlorinated solvents, with the formation of the dimeric species $\{[2\text{-}(Me_2NCH_2)C_6H_4]_2SnSe\}_2$ (**10-a**), $\{[2\text{-}(Me_2NCH_2)C_6H_4](Me)SnSe\}_2$ (**11-a**) and $\{[2\text{-}(Me_2NCH_2)C_6H_4](^nBu)SnSe\}_2$ (**12-a**), for which the single crystal X-ray diffraction studies showed hypercoordination, *i.e.* *12−Sn−6* (**10-a**) and *10−Sn−5* (**11-a** and **12-a**)species, determined by intramolecularly coordinated pendant arms and dimerization by bridging selenium atoms.
- The molecular structures of compounds **15** and **16,** were studied with X-ray diffraction and they show hypercoordination due to N→Sn intramolecular interactions, namely molecular *10−Sn−5* species;
- The thermogravimetric studies for compounds **11**, **15**, **16** and **19** suggested a significant volatility in inert atmosphere, which recommends them as potential candidates for CVD processes;
- The experiments under a flow of synthetic air suggested the possibility of obtaining tin selenides under certain conditions;
- Compounds **3**, **10**, **15**, **16**, **19** and **20** showed a promissing antiproliferative activity against the murine melanoma B16.F10 cell line.

6. References

1 A. Mason, W. Powell, H. A. Bankoff, R. Mathur, M. Price, A. Bulatović, V. Filipović, *J. Archaeol. Sci.*, **2020**, *122*, 105181.

2 J. Otera, M. Biesemans, V. Pinoie, K. Poelmans, R. Willem, A. G. Davies, K. Pannell, *Tin Chemistry: Fudamentals, Frontiers, and Applications*, M. Gielen, A. G. Davies, K. Pannell, K. Tiekink, E.R.T., Eds., John Wiley & Son, Ltd.: New York, NY, USA,2008.

3 A. Ross, *Ann. N. Y. Acad. Sci.*, **1965**, *125*, 107–123.

4 M. T. Berard in C. E. Wilkes, J. W. Summers, C. A. Daniels (Eds.), *PVC Handbook*, Hanser Pubn., **2005**.

5 P. Atkins, T. Overton, J. Rourke, M. Weller, F. Armstrong, M. Hagerman, *Inorganic Chemistry*, p. 371, 5th Edition, Oxford Univ. Press, UK, **2006**.

6 H. Mou, W. Xiao, C. Miao, R. Li, L. Yu, *Front. Chem.*, **2020**, *8*, 1–14.

7 V. Farina, V. Krishnamurthy, W. J. Scott, *The Stille Reaction*, in A. Leo (Ed.) *Organic Reactions*, vol. 50, John Wiley& Sons, **1997**.

8 A. G. Davies, *Organotin Chemistry*, Ch. 22, p. 373, Wiley-VCH, **2004**.

9 T. Wirth (Ed.), *Organoselenium Chemistry - Modern Developments in Organic Synthesis*, Top. Curr. Chem., vol. 208, Springer, Berlin, **2000**.

10 V. K. Jain, K. I. Priyadarsini, *Organoselenium Compounds in Biology and Medicine: Synthesis, Biological and Therapeutic Treatments*, Eds.; RSC Publishing: London, UK, **2018**.

11 J. J. Berzelius, *Afh. i Fys. Kemi och Miner.*, **1818**, *VI*, 42–144.

12 L. Flohe, W. A. Günzler, H. H. Schock, *FEBS Lett.*, **1973**, *32*, 132–134.

13 K. P. Bhabak, G. Mugesh, *Acc. Chem. Res.*, **2010**, *43*, 1408–1419.

14 A. Pöllnitz, A. Rotar, A. Silvestru, C. Silvestru, M. Kulcsar, *J. Organomet. Chem.*, **2010**, *695*, 2486–2492.

15 R. Kaur, H. B. Singh, R. P. Patel, *J. Chem. Soc. - Dalton Trans.*, **1996**, 2719–2726.

16 A. S. Hodage, P. P. Phadnis, A. Wadawale, K. I. Priyadarsini, V. K. Jain, *Org. Biomol. Chem.*, **2011**, *9*, 2992–2998.

17 E. E. Alberto, V. D. Nascimento, A. L. Braga, *J. Braz. Chem. Soc.*, **2010**, *21*, 2031–2041.

18 V. Nascimento, N. L. Ferreira, R. F. S. Canto, K. L. Schott, E. P. Waczuk, L. Sancineto, C. Santi, J. B. T. Rocha, A. L. Braga, *Eur. J. Med. Chem.*, **2014**, *87*, 131–139.

19 K. P. Bhabak, G. Mugesh, *Chem. - An Asian J.*, **2009**, *4*, 974–983.

20 K. Selvakumar, P. Shah, H. B. Singh, R. J. Butcher, *Chem. - A Eur. J.*, **2011**, *17*, 12741–12755.

21 G. Mugesh, A. Panda, H. B. Singh, N. S. Punekar, R. J. Butcher, *J. Am. Chem. Soc.*, **2001**, *123*, 839–850.

22 A. J. Mukherjee, S. S. Zade, H. B. Singh, R. B. Sunoj, *Chem. Rev.*, **2010**, *110*, 4357–4416.

23 C. W. Nogueira, J. B. T. Rocha, *Springer Verlag*, **2011**, *85*, 1313–1359.

24 F. Kumakura, B. Mishra, K. I. Priyadarsini, M. Iwaoka, *European J. Org. Chem.*, **2010**, 440–445.

25 D. Krasowska, N. Iraci, C. Santi, J. Drabowicz, M. Cieslak, J. Kaźmierczak-Barańska, M. Palomba, K. Królewska-Golińska, J. Magiera, L. Sancineto, *Molecules,* **2019**, *24*, 2914.

26 W. G. Salgueiro, M. C. D. F. Xavier, L. F. B. Duarte, D. F. Câmara, D. A. Fagundez, A. T. G. Soares, G. Perin, D. Alves, D. S. Avila, *Eur. J. Med. Chem.*, **2014**, *75*, 448–459.

27 M. Iwaoka, S. Tomoda, *J. Am. Chem. Soc.*, **1994**, *116*, 2557–2561.

28 K. P. Bhabak, G. Mugesh, *Chem. - A Eur. J.*, **2007**, *13*, 4594–4601.

29 M. Pellei, C. Santini, G. G. Lobbia, F. Cantalamessa, C. Nasuti, M. D. Prinzio, R. Gabbianelli, G. Falcioni, *Appl. Organomet. Chem.*, **2005**, *19*, 583–589.

30 M. Gielen, *Appl. Organometal. Chem.*, **2002**, *16*, 481–494.

31 M. Hébert, P. Petiot, E. Benoit, J. Dansereau, T. Ahmad, A. Le Roch, X. Ottenwaelder, A. Gagnon, *J. Org. Chem.*, **2016**, *81*, 5401–5416.

32 A.-A. Someşan, S. M. Vieriu, A. Crăciun, C. Silvestru, P. Chiroi, A. Nutu, A. Jurj, R. Lajos, I. Berindan-Neagoe, R. A. Varga, *Appl. Organomet. Chem.*, **2022**, *36*, 1–19.

33 P. Švec, Z. Růžičková, P. Vlasák, J. Turek, F. De Proft, A. Růžička, *J. Organomet. Chem.*, **2016**, *801*, 14–23.

34 A. Ruzicka, V. Pejchal, J. Holecek, A. Lycka, K. Jacob, *Collect. Czech. Chem. Commun.*, 63, 977–989.

35 R. A. Varga, M. Schuermann, C. Silvestru, *J. Organomet. Chem.*, **2001**, *623*, 161–167.

36 C. Coza, A. Stegarescu, R. Şuteu, A. Silvestru, *J. Organomet. Chem.*, **2015**, *777*, 71–80.

37 T. P. Lockhart, W. F. Manders, *J. Am. Chem. Soc.*, **1987**, *109*, 7015–7020.

38 I. Wharf, M. G. Simard, *Inorganica Chim. Acta*, **1998**, *282*, 30–37.

39 B. Hellman, H. Vaghef, B. Bostrijm, *DNA Repair*, **1995**, *336*, 123–131.

40 M. A. Franzman, C. W. Schlenker, M. E. Thompson, R. L. Brutchey, *J. Am. Chem. Soc.*, **2010**, *132*, 4060–4061.

41 N. R. Mathews, *Sol. Energy*, 2012, **86**, 1010–1016.

42 R. K. Sharma, G. Kedarnath, A. Wadawale, C. A. Betty, B. Vishwanadh, V. K. Jain, *Dalton Trans.*, **2012**, *41*, 12129–12138.

43 A. Tyagi, G. Kedarnath, A. Wadawale, A. Y. Shah, V. K. Jain, B. Vishwanadh, *RSC Adv.*, **2016**, *6*, 8367–8376.

44 G. Karmakar, K. K. Halankar, A. Tyagi, B. P. Mandal, A. P. Wadawale, G. Kedarnath, A. P. Srivastava, V. Singh, *Dalton Trans.*, **2021**, *50*, 15730–15742.

45 T. P. Lockhart, F. Davidson, *Organometallics*, **1987**, *6*, 2471–2478.

46 R. Y. Tan, H. Bin Song, L. F. Tang, *J. Organomet. Chem.*, **2006**, *691*, 5964–5969.

47 A. Molter, G. N. Kaluerović, H. Kommera, R. Paschke, T. Langer, R. Pöttgen, F. Mohr, *J. Organomet. Chem.*, **2012**, *701*, 80–86.

48 Y. Y. Zhang, R. F. Zhang, S. L. Zhang, S. Cheng, Q. L. Li, C. L. Ma, *Dalton Trans.*, **2016**, *45*, 8412–8421.

49 R. F. Zhang, J. Ru, Z. X. Li, C. L. Ma, J. P. Zhang, *J. Coord. Chem.*, **2011**, *64*, 4122–4133.

50 S. Wen, H. Pan, Y. Zheng, *J. Mater. Chem. C*, **2015**, *3*, 3714–3721.

51 D. H. Lee, C. M. Park, *ACS Appl. Mater. Interfaces*, **2017**, *9*, 15439–15448.

52 M. M. Amin, S. Ali, S. Shahzadi, S. K. Sharma, K. Qanungo, *J. Coord. Chem.*, **2011**, *64*, 337–350.

53 K. N. D. Oliveira, V. Andermark, L. A. Onambele, G. Dahl, A. Prokop, I. Ott, *Eur. J. Med. Chem.*, **2014**, *87*, 794–800.

54 R. N. Reddi, P. V. Malekar, A. Sudalai, *Tetrahedron Lett.*, **2013**, *54*, 2679–2681.

55 G. Mugesh, W.-W. D. Mont, H. Sies, *Chem. Rev.*, **2001**, *101*, 2125–2179.

56 R. A. Popa, E. Licarete, M. Banciu, A. Silvestru, *Appl. Organomet. Chem.*, **2018**, *32*, 1–10.

57 A. Meller, H. Hoppe, W. Maringgele, A. Haase, M. Noltemeyer, *Organometallics*, **1998**, *17*, 123–124.

58 R. A. Varga, A. Rotar, M. Schürmann, K. Jurkschat, C. Silvestru, *Eur. J. Inorg. Chem.*, **2006**, *2*, 1475–1486.

59 K. Angermund, K. Jonas, C. Krueger, J. L. Latten, Y.-H. Tsay, *J. Org. Chem.*, **1988**, *353*, 17–25.

60 B. Wrackmeyer, M. Vosteen, W. Storch, *J. Mol. Struct.*, **2002**, *603*, 177–184.

61 J. C. Martins, M. Biesemans, R. Willem, *Prog. Nucl. Magn. Reson. Spectrosc.*, **2000**, *36*, 271–322.

62 T. P. Lockhart, W. F. Manders, *Inorg. Chem.*, **1986**, *25*, 892–895.

63 T. P. Lockhart, W. F. Manders, J. J. Zuckerman, *J. Am. Chem. Soc.*, **1985**, *107*, 4546–4547.

64 J. Holeček, A Lycka, *Inorg. Chim. Acta.*, **1986**, *118*, 15.

65 J. Holeček, K. Handlíř, M. Nádvorník, *Z. Chem.*, **1990**, *30*, 265–266.

66 S. Alvarez, *Dalton Trans.*, **2013**, *42*, 8617–8636.

67 A. W. Addison, T. N. Rao, J. Reedijk, J. van Rijn, G. C. Verschoor, *J. Chem. Soc. Dalton Trans.*, **1984**, *3*, 1349–1356.

68 N. G. Connelly, T. Damhus, R. M. Hartshorn, A. T. Hutton (Eds.), *Nomenclature of Inorganic Chemistry, IUPAC Recommendations 2005*, RSC Publishing, Cambridge, **2005**.

69 C. W. Perkins, J. C. Martin, A. J. Arduengo, W. Lau, A. Alegría, J. K. Kochi, *J. Am. Chem. Soc.*, **1980**, *102*, 7753–7759.

70 G. Van Koten, J. Jastrzebski, J. G. Noltes, *J. Org. Chem.*, **1979**, *177*, 283–292.

71 R. Rippstein, G. Kickelbick, U. Schubert, *Monatsh. Chem.*, **1999**, *130*, 385–399.

72 R. A.Varga, K. Jurkschat, C. Silvestru, *Eur. J. Inorg. Chem.*, **2008**, 708–716.

73 M. Iwaoka, S. Tomoda, *J. Am. Chem. Soc.*, **1996**, *118*, 8077–8084.

74 B. Wrackmeyer, H. E. Maisel, W. Milius, M. Herberhold, *J. Organomet. Chem.*, **2003**, *680*, 271–280.

75 A. L. Spek, *Acta Cryst.*, **2009**, *D65*, 148–155.

76 A. L. Spek, *Acta Crystallogr. Sect. C*, **2015**, *C71*, 9–18.

77 A. Chaudhary, A. K. Singh, R. V. Singh, *J. Inorg. Biochem.*, **2006**, *100*, 1632–1645.

78 B. E. G. Lucier, V. V. Terskikh, J. Guo, J. L. Bourque, S. L. McOnie, J. A. Ripmeester, Y. Huang, K. M. Baines, *Inorg. Chem.*, **2020**, *59*, 13651–13670.

79 A. Eichhöfer, J.-J. Jiang, H. Sommer, F. Weigend, O. Fuhr, D. Fenske, C.-Y. Su, G. Buth, *Eur. J. Inorg. Chem.*, **2010**, *3*, 410–418.

80 J. R. Thompson, I. Y. Ahmet, A. L. Johnson, G. Kociok-Köhn, *Eur. J. Inorg. Chem.*, **2016**, 4711–4720.

81 A. Tyagi, G. Karmakar, A. Wadawale, A. Y. Shah, G. Kedarnath, A. P. Srivastava, V. Singh, V. K. Jain, *J. Organomet. Chem.*, **2018**, *873*, 15–21.

82 S. S. Sadhu, S. Wang, R. K. Averineni, T. Seefeldt, Y. Yang, X. Guan, *Melanoma Res.*, **2016**, *26*, 572–579.

83 J. H. P Novák, Z Padělková, L Kolářová, I Císařová, A Rûžička, *Appl. Organomet. Chem.*, **2005**, *19*, 1101–1108.

84 A.-A. Someșan, R. A. Varga, C. Silvestru, *Rev. Roum. Chim.*, **2014**, *59*, 931–938.

85 A. L. J. Holeček, M. Nádvorník, K. Handlír, *J. Organomet. Chem.*, **1986**, *315*, 299–308.

86 J. Holeček, A. Lycka, K. Handlír, *J. Chem. Soc., Chem. Commun.*, **1990**, *55*, 1193–1207.

87 MestReNova, Mestrelab Research S.L., Feliciano Barrera 9B – Bajo, 15706 Santiago de Compostela, Spain, http://mestrelab.com.

88 Xcalibur™ Software, Thermo Fisher Scientific, 168 Third Avenue, Waltham, MA USA, https://www.thermofisher.com.

89 G. M. Sheldrick, *Acta Crystallogr. Sect. C*, **2015**, *C71*, 3–8.

8. Results dissemination

List of articles

1. Melinda Tamas, Alexandra Pop and Anca Silvestru, Homoleptic triorganoatin(IV) organoselenolates of type $R_3Sn(SeCH_2CH_2pz)$, *Rev. Roum. Chim.*, **2025**, *in press*.
2. Melinda Tamas, Roxana A. Butuza, Monica Dan, Anca Silvestru, Diorganotin(IV) Complexes of Organoselenolato Ligands with Pyrazole Moieties-Synthesis, Structure and Properties, *Molecules*, **2025**, *in press*.

List of conferences

1. Melinda Tamas, Raluca Mitea, Anca Silvestru, *Diorganochalcogenides with alcoxo functionalities and their silver(I) complexes*. Poster presentation at the 3rd Young Researchers' International Conference on Chemistry and Chemical Engineering (YRICCCE III), 4 – 5 June 2021, Cluj-Napoca, Romania.
2. Melinda Tamas, Raluca Mitea, Anca Silvestru, *Diorganochalcogenides with alcoxo functionalities*. Poster presentation at the National Chemistry Conference, 36th edition, 4 – 7 October 2022, Călimănești-Căciulata, Romania.
3. Melinda Tamas, Roxana-Alexandra Butuza, Anca Silvestru, *Diorganotin(IV) complexes with organoselenolato ligands.* Poster presentation at the 4th Young Researchers' International Conference on Chemistry and Chemical Engineering (YRICCCE IV), 1 – 3 June 2023, Debrecen, Hungary.
4. Melinda Tamas, Anca Silvestru, *New series of diorganotin(IV) complexes with organoselenolato ligands*. Oral presentation at the National Chemistry Conference, 37th edition, 25 – 27 September 2024, Targoviste, Romania.
5. Melinda Tamas, Anca Silvestru, *Structural aspects in organotin(IV) selenolates*. Oral presentation at the 5th Young Researchers' International Conference on Chemistry and Chemical Engineering (YRICCCE V), 8-10 May 2025, Cluj-Napoca, România.